Non canonical scaffold-type ligase complex mediates protein UFMylation

Joshua J. Peter[1], Helge M. Magnussen[1], Paul Anthony DaRosa[2], David Millrine[1], Stephen P Matthews[1], Frederic Lamoliatte[1], Ramasubramanian Sundaramoorthy[3], Ron R Kopito[2] and Yogesh Kulathu[1]*

Affiliations –

[1] Medical Research Council Protein Phosphorylation & Ubiquitylation Unit (MRC-PPU), School of Life Sciences, University of Dundee, Dundee DD1 5EH, UK.

[2] Department of Biology, Stanford University, Stanford, CA 94305, USA

[3] Centre for Gene Regulation and Expression, School of Life Sciences, University of Dundee, Dundee DD1 5EH, UK

***corresponding author –**

Dr Yogesh Kulathu, Medical Research Council Protein Phosphorylation & Ubiquitylation Unit (MRC-PPU), School of Life Sciences, University of Dundee, Dow Street, Dundee DD1 5EH, UK.

Tel: +44 1382 388163; E-mail: ykulathu@dundee.ac.uk

Running Title: Mechanism of UFMylation

Abstract

Protein UFMylation is emerging as a posttranslational modification essential for endoplasmic reticulum and cellular homeostasis. Despite its biological importance, we have a poor understanding of how UFM1 is conjugated onto substrates. Here, we use a rebuilding approach to define the minimal requirements of protein UFMylation. We find that the reported E3 ligase UFL1 is inactive on its own and identify UFBP1 to bind UFL1 to form an active E3 ligase complex. While UFC1 is an intrinsically Cys-reactive E2, we do not identify any catalytic cysteines on UFL1/UFBP1, suggesting a scaffold-type E3 ligase mechanism. Interestingly, the E3 ligase complex consists of winged-helix (WH) domain repeats that activate UFC1 for aminolysis. We identify the adaptor protein CDK5RAP3 to bind to and regulate E3 ligase activity potentially by preventing off-target UFMylation. In summary, our work identifies the minimal requirements for UFMylation and reveals regulatory principles of this atypical E3 ligase complex.

Main

UFM1 is a ubiquitin-like (Ubl) modifier that contains the characteristic β-grasp fold found in all UBLs and is highly conserved in multicellular eukaryotes [1,2]. Like other UBLs, UFM1 is covalently attached to lysine residues on substrates via an enzymatic cascade involving an E1 activating enzyme, UFM1-activating enzyme 5 (UBA5), E2 conjugating enzyme, UFM1-conjugating enzyme 1 (UFC1), and an E3 ligase, UFM1 E3 ligase 1 (UFL1) [3,4]. Recent studies have identified the ribosomal protein RPL26 to be the principal target of UFMylation which plays a critical role in endoplasmic reticulum (ER) homeostasis [5–7]. Besides ER associated roles, UFMylation has also been implicated in other cellular processes including protein translation, DNA damage response and nuclear receptor mediated transcription [8–13]. Further, loss of or mutation of components of the UFMylation machinery has been linked to many diseases such as cancer, type-2 diabetes, neurological disorders and cerebellar ataxia, where failure of ER homeostasis and protein quality control could be one of the major contributing factors [12,14–17]. Indeed, UFMylation is an essential posttranslational modification for animal development as loss of UFM1 or any of the UFMylation enzymes results in failure of erythropoiesis and embryonic lethality [18–21].

UFM1 is expressed in a precursor form consisting of 85 amino acids. It is then post-translationally processed by UFM1-specific proteases (UFSPs) which cleave off the last two residues at the C-terminus to generate mature UFM1 that contains an exposed C-terminal glycine, Gly^{83} [22]. Mature UFM1 is activated by the E1, UBA5 via the formation of a high-energy thioester bond between Cys^{250} of UBA5 and Gly^{83} of UFM1 [3,23]. Activated UFM1 is then transferred from UBA5 on to the catalytic Cys^{116} of UFC1 [3,24]. UFC1 has a canonical UBC fold and in addition an N-terminal helical extension whose function is not known [25,26]. UFC1 lacks many of the features conserved in many E2s such as the catalytic HPN motif which suggests unique modes of action and regulation. Further, ubiquitin (Ub) E2 enzymes such as UBE2D3 associate with Ub via a backside interaction which mediates E2 dimerization and processivity of polyUb formation [27,28]. For UFC1, it is unknown if similar mechanisms exist to regulate its activity as detailed biochemical characterization is lacking.

71 UFL1 is the only E3 ligase identified to date in the UFMylation pathway catalysing the
72 final step of transfer of UFM1 from UFC1 to substrates [29]. Indeed, loss of UFL1 results
73 in loss of UFMylation and mice lacking Ufl1 phenocopy loss of UFM1 exhibiting failure
74 in haematopoiesis and embryonic lethality suggesting that it could be the main E3
75 ligase [30]. While data implying UFL1 is the E3 ligase stem from knockout studies and
76 overexpression studies, direct biochemical evidence demonstrating that UFL1 is an
77 E3 ligase is insufficient [24]. Consequently, the mechanism of how UFL1 functions as
78 an E3 ligase is also not understood. In general, E3 ligases are classified either as
79 scaffold-type ligases that bring together a UBL-charged E2 with substrate for direct
80 transfer of the UBL from the E2 on to substrate, or as Cys-dependent enzymes where
81 the UBL is first transferred from the E2 to the catalytic Cys of the E3 for subsequent
82 transfer to the substrate [31]. Examples of scaffold-type E3s are RING family ligases
83 and RANBP2 whereas HECT, RBR and RCR enzymes typify the latter type [32–36].
84 Intriguingly, UFL1 does not possess any conserved sequence or domain features
85 found in known E3 ligases. Hence it is not clear if UFL1 is a Cys-dependent E3 enzyme
86 or uses a scaffolding mechanism.

87 UFL1 is predominantly found anchored at the ER through its interaction with an
88 adaptor protein, DDRGK1/UFBP1 (UFM1 binding protein-1) which has also been
89 suggested to be one of the main substrates of UFL1 [29,37]. UFBP1 localizes to the ER
90 membrane via an N-terminal transmembrane segment and its function is unclear [5].
91 Intriguingly, loss of UFBP1 affects the stability and expression levels of UFL1 [20,29,37].
92 CDK5RAP3 is another poorly characterized protein commonly associated with UFL1.
93 Several anecdotal reports have led to speculations that UFL1, UFBP1 and
94 CDK5RAP3 together form an E3 ligase complex [24,38]. Only a handful of substrates of
95 UFL1 have been identified to date and many of them are ER localized [38,39]. In addition
96 to monoUFMylation, polyUFM1 chains can be assembled which are mainly linked via
97 K69 [12]. In the Ub system, the type of polyUb linkage formed is generally dictated by
98 the last enzyme in the cascade that forms a thioester linkage with Ub before transfer
99 to substrate. Scaffold-type E3s such as RING E3 ligases bind to charged E2 (E2~Ub)
100 to mediate transfer of Ub onto substrate, and hence the E2 enzymes are thought to
101 determine the linkage type assembled. In contrast, catalytic Cys containing E3 ligases
102 form an E3~Ub thioester intermediate and dictate the linkage type formed [31,34].

Given the lack of understanding of the molecular mechanism underpinning the UFM1 conjugation machinery and the mechanisms governing its regulation, here we adopt a rebuilding approach with purified components to fully reconstitute UFMylation *in vitro*. Using this reductionist approach, we reveal that UFL1 on its own is an unstable protein that cannot support UFMylation. We demonstrate that UFL1 together with UFBP1 forms a functional hetrodimeric E3 ligase complex and provide in depth biochemical characterization of the ligase complex. Structure prediction using Alphafold provides an explanation for the underlying reason for complex formation between UFL1 and UFBP1 and offers a rational framework for making truncations which help establish the minimal regions on UFL1 and UFBP1 essential for ligase activity. Parallel investigations of UFC1 reveal that it is an intrinsically Cys reactive enzyme that is activated by the UFL1/UFBP1 ligase complex for aminolysis. Our analyses reveal UFL1/UFBP1 to be a scaffold-type E3 ligase. Further, we identify CDK5RAP3 to bind to the E3 ligase complex and inhibit UFMylation by preventing discharge of UFM1 from UFC1. Importantly, by reconstituting UFMylation of ribosomes *in vitro,* we find that CDK5RAP3 has a regulatory function as it restricts UFMylation towards *bona fide* substrates and lysine selectivity. Lastly, we identify an N-terminal helical extension on UFC1 to have an inhibitory role that is required by CDK5RAP3 to restrain UFMylation. Our mechanistic insights describe an atypical E3 ligase complex and provide a foundation for investigating the catalytic mechanism, regulation, and substrate specificity of this E3 ligase complex.

125 **Results**

126 **UFC1 has intrinsic cysteine reactivity**

127 The interaction of UFC1 with UBA5 and how UFM1 is transferred from UBA5 to the
128 catalytic Cys is reasonably well understood [23,24,40–42]. We therefore focussed on
129 subsequent events and first analysed the intrinsic reactivity and stability of
130 UFC1~UFM1 (~ denotes the thioester bond between $UFM1^{G83}$ and $UFC1^{C116}$) in
131 comparison to the well characterized ubiquitin E2s, UBE2D3 and UBE2L3 [43]. Intrinsic
132 reactivity of E2s assayed using free amino acids can give insights into the ability of
133 E2s to transfer UBLs onto substrates and can provide clues about the type of E3 ligase
134 they work with and even the nature of the substrate [27,36]. For instance, E2s such as
135 UBE2D3 which function together with RING/scaffold like E3 ligases are capable of
136 aminolysis and are therefore reactive towards the free amino acid Lys (**Fig 1A, B**) [43].
137 On the other hand, UBE2L3 which functions only with Cys-dependent E3 ligases is
138 incapable of aminolysis and lacks reactivity to free Lys on its own (**Fig 1B**) [43]. When
139 discharge of UFM1 from UFC1~UFM1 onto free amino acids was analysed, we
140 observed preferential discharge onto Cys while no discharge was observed in the
141 presence of Lys, Arg, Ser and Thr (**Fig 1C**). Under the same experimental conditions,
142 UBE2D3 discharged Ub in the presence of both Cys and Lys (**Fig 1C, Fig S1A**).
143 Further, using increasing concentrations of free Lys or with prolonged incubation in a
144 time course, we find that UFC1 has negligible Lys reactivity which is similar to UBE2L3
145 (**Fig 1D-E, S1B**). These results suggest that UFC1 has intrinsic Cys reactivity and may
146 work with Cys-dependent E3 ligases.

147 **UFL1 together with UFBP1 forms an active E3 ligase complex**

148 To analyse how UFC1 works together with the E3 ligase UFL1 to transfer UFM1, we
149 aimed to reconstitute UFMylation using UFL1. We expressed 6xHis-UFL1 in *E. coli*
150 and purified it by affinity chromatography as the first step. Subsequent size exclusion
151 chromatography (SEC) analysis indicated UFL1 to elute in the void fraction suggesting
152 formation of soluble aggregates (**Fig S2A**). Our attempts to prevent aggregation by
153 incorporating different solubility enhancing tags at the N-terminal or C-terminal ends
154 of UFL1 or with different buffers and additives were unsuccessful. We therefore
155 reasoned that UFL1 might require additional binding partners for its stability and

156 activity. Indeed, several studies have shown that expressing subunits of protein
157 complexes individually may result in aggregation [44–46]. To identify binding partners of
158 UFL1, we performed Yeast Two Hybrid (Y2H) screening using a cDNA library derived
159 from human placenta as prey (**Fig S2B**). Surprisingly, only four hits were identified
160 with UFBP1 being the most significant interactor. We therefore wondered if co-
161 expressing UFBP1 with UFL1 might confer solubility and stability to UFL1. To achieve
162 this, we used a co-expression system to express full-length UFL1 together with UFBP1
163 lacking its transmembrane sequence and purified the ligase complex with three
164 enrichment steps (**Fig S2C**). Indeed, UFL1 co-expressed with UFBP1 lacking its N-
165 terminal transmembrane segment (UFL1/UFBP1) is soluble, well behaved and no
166 longer formed soluble aggregates in SEC (**Fig 2A**). We confirmed the formation of a
167 stable UFL1/UFBP1 complex by analysing its precise molecular mass using a mass
168 photometer [47] and SEC-MALS (**Fig 2B, S2D**). This revealed UFL1/UFBP1 to have a
169 mass of 126 kDa which corresponds to that of a heterodimeric complex. Of note, the
170 mass photometry measurements are performed at low nanomolar concentrations
171 highlighting the stable nature of the complex.

172 Having obtained soluble UFL1/UFBP1 complexes, we next tested the catalytic activity
173 of UFL1 expressed alone and in complex with UFBP1 using *in vitro* UFMylation assays
174 containing UBA5, UFC1 and UFM1. Whereas UFL1 on its own did not show any
175 appreciable activity, the UFL1/UFBP1 complex is an active ligase as evidenced by the
176 formation of multiple UFMylated products and UFL1 autoUFMylation (**Fig 2C**). To
177 check if UFL1/UFBP1 was capable of UFMylating substrates *in vitro*, we used
178 TRIP4/ASC1, a protein reported to be UFMylated in cells [12]. Indeed, UFL1/UFBP1 can
179 efficiently UFMylate TRIP4 *in vitro* (**Fig 2C**). Intriguingly, exogenous addition of
180 purified UFBP1 to UFL1 expressed on its own does not change the elution profile of
181 UFL1 to match that of co-expressed UFL1/UFBP1 or restore its E3 ligase activity (**Fig**
182 **S2E-F**). Taken together, these results show that UFL1 and UFBP1 form an obligate
183 heterodimer required for E3 ligase activity.

184 Since polyUFMylated products are formed in UFMylation reactions, we next analysed
185 the reaction products by mass spectrometry to determine the linkage types
186 assembled. Interestingly, LC/MS analyses revealed that the polyUFM1 chains are

187 formed which are predominantly linked via K69 with some K3 and K7 linkages also
188 observed (**Fig 2D**). To validate these observations, we generated a series of K-R
189 mutants where every Lys in UFM1 was individually mutated to Arg. While mutation of
190 K3, K7, K19, K34 or K41 to Arg did not affect overall UFMylation, UFM1 K69R resulted
191 in near complete loss of polyUFMylated species and unanchored diUFM1, closely
192 resembling reactions with UFM1 K0 in which all Lys were mutated to Arg (**Fig 2E** lanes
193 7&8**, S2G**). Interestingly, western blotting for UFL1 revealed only monoUFMylated
194 UFL1 in the presence of UFM1 K69R suggesting that UFL1 autoUFMylation involves
195 formation of polyUFM1 chains on UFL1 that are linked via K69 (**Fig 2E**). We next
196 generated K_{only} UFM1 mutants that contain only a single Lys while all others are
197 mutated to Arg. UFMylation assays using these mutants confirm that K69 is the
198 preferred linkage type assembled (**Fig 2F**). Single Lys-retaining mutants all abrogate
199 polyUFMylation formation comparably to UFM1 K0 with the sole exception of K69-only
200 UFM1 (**Fig 2F**). In reactions with UFM1 K69R or K0, mainly monoUFMylated products
201 corresponding to modified UFL1, UFBP1 and UFC1 are formed. In summary, our
202 reconstitution experiments reveal that UFL1 together with UFBP1 forms an active E3
203 ligase complex that can efficiently UFMylate substrates and assemble polyUFM1
204 chains that are K69-linked.

205 **UFL1/UFBP1 is a scaffold type E3 ligase complex activating UFC1 for aminolysis**

206 Our analyses find that UFC1 is an intrinsically Cys-reactive E2 suggesting that UFL1
207 may be a Cys-dependent enzyme (**Fig 1**). The N-terminal region of UFL1 contains
208 four Cys residues and sequence analysis show that all four vary in their degree of
209 conservation with C32 being the most conserved (**Fig 3A**). Based on analysis of
210 predicted folding propensity (**Fig S3A**) and secondary structure prediction, we made
211 a C-terminal truncation of UFL1, $UFL1^{1-410}$, which when expressed on its own formed
212 soluble aggregates like full length UFL1 and required co-expression of UFBP1 to
213 obtain a heterodimeric complex (**Fig S3B**). Importantly, this $UFL1^{1-410}$/UFBP1 complex
214 is an active ligase **(Fig S3C**). To identify the catalytic Cys in UFL1, we mutated each
215 Cys individually to Ala in the $UFL1^{1-410}$/UFBP1 complex. To our surprise, *in vitro*
216 UFMylation assays showed that none of the single mutants had any impact on the
217 autoUFMylation activity of UFL1 or UFMylation of substrates implying that UFL1 does
218 not contain a catalytic Cys (**Fig 3B**). Since UFBP1 does not have any Cys residues,

219 these results suggest that the UFL1/UFBP1 ligase complex may instead employ a
220 scaffolding mechanism to transfer UFM1 on to substrate. Further, we do not observe
221 any transthiolation products of UFL1/UFBP1 **(Fig S3D)**.

222 This raises the possibility that the UFL1/UFBP1 ligase complex could induce
223 aminolysis of UFC1~UFM1. Hence, we compared discharge of UFM1 from
224 UFC1~UFM1 onto Lys in the absence and presence of the ligase complex. Whereas
225 UFC1 does not discharge UFM1 onto Lys on its own, UFM1 was readily discharged
226 onto Lys in the presence of UFL1/UFBP1 (**Fig 3D**). Based on these observations, we
227 suggest that UFL1/UFBP1 functions as a scaffold-type E3 ligase that binds to charged
228 UFC1 to promote aminolysis.

229 While inefficient, UFC1 on its own can assemble free UFM1 chains which is
230 significantly enhanced in the presence of the UFL1/UFBP1 ligase complex (**Fig S3E-**
231 **F**). Interestingly, UFC1 assembles mainly K69 linkages (**Fig 3D**) and this linkage
232 specificity is maintained in the presence of UFL1/UFBP1 (**Fig 2D**). Of note, this reveals
233 that the linkage specificity is determined by the E2 and is not altered by the E3 ligase
234 complex, a feature commonly observed in ubiquitin RING E3 ligases [34,48,49]. These
235 results further strengthen our conclusion that UFL1/UFBP1 is a scaffold-type ligase
236 complex.

237 **Tandem WH domains of UFL1/UFBP1 constitute minimal E3 ligase**

238 As UFL1 does not have any obvious sequence or domain features found in any of the
239 known E3 ligases, we attempted to define the minimal catalytic region on UFL1. As
240 our efforts to determine the structure of this complex were not successful, we used the
241 recently released AlphaFold pipeline to predict the structure (**Fig 4A**) [50]. Structure
242 prediction of the complex had good predicted aligned error (PAE) scores (**Fig S4A**)
243 and shows UFL1 and UFBP1 form a heterodimer (**Fig 4A-B**). Interestingly, UFL1 is
244 predicted to contain 5 winged-helix (WH) domain repeats and a C-terminal helical
245 domain (**Fig 4A** blue, **S4B-C**). The WH repeats are arranged such that a helix from
246 each WH domain forms a helical backbone. The fifth WH domain on UFL1 is followed
247 by a disordered region that extends into a stack of α-helices at its C-terminus which
248 we refer to as CTR (C-Terminal Region). These WH domains could be classified as
249 PCI-like WH domains, named so because it is commonly found in components of the

250 proteasome lid, the COP9 signalosome and the eukaryotic translation initiator, eIF3
251 [51,52]. In addition, UFL1 is predicted to have an N-terminal helix (1-25) followed by a
252 partial or hemi-WH domain (pWH) (**Fig 4B,** blue). Following the transmembrane
253 segment at its N-terminus, UFBP1 has a long coiled-coil region which we refer to as
254 NTR (N-Terminal Region) followed by a WH (WH') domain and ends with a hemi-WH
255 domain (pWH') (**Fig 4B, teal**). Interestingly, the hemi-WH (pWH) from UFL1
256 complements the hemi WH (pWH') from the C-terminus of UFBP1 to form a complete
257 WH domain (**Fig 4B**), thus providing an explanation to why UFBP1 is required to
258 stabilize UFL1. Further support to this model is provided by our Y2H screen which
259 identifies the region spanning 268-298, i.e. the C-terminal portion of UFBP1 to interact
260 with UFL1. Superposition of the WH domains of UFL1 and UFBP1 reveal them to have
261 identical folds except for a β-strand which is lacking in the composite WH domain (**Fig**
262 **S4D-E**). The coiled-coil nature of UFBP1 and the helical backbone of UFL1 may
263 explain the unusual migration of UFL1/UFBP1 by SEC. To validate the predicted
264 structure of the UFL1/UFBP1 complex, we deleted the N-terminal helix along with
265 pWH of UFL1 and checked for complex formation with UFBP1. Indeed we failed to
266 obtain any protein upon deletion of this region of UFL1. Likewise, removal of C-
267 terminal pWH domain of UFBP1 also resulted in poor expression, highlighting the
268 importance of the formation of the composite WH (pWH-pWH') domain for complex
269 formation and protein stability.

270 Guided by the insights from the Alphafold predictions, we made additional truncations
271 to map the minimal catalytic domain of the ligase complex (**Fig 4C**). The truncated
272 complexes expressed well and were purified to homogeneity (**Fig S3F**). We first
273 analysed the ability of the different truncated complexes to promote discharge of
274 UFM1 from UFC1~UFM1 onto Lys. This revealed that all the truncations tested could
275 discharge UFM1 and the smallest region able to promote discharge contains one WH
276 domain each from UFL1 and UFBP1 and the composite WH domain (**Fig 4D, S5A-B**).

277 We then monitored the ability of the different UFL1/UFBP1 complexes to bind to UFC1
278 for which we performed analytical SEC of the different UFL1/UFBP1 constructs with
279 UFC1 on its own or a stable non-reactive UFC1$^{-O-UFM1}$ conjugate where UFM1 is linked
280 to C116S via an oxyester bond (**Fig S5 C-D**). UFC1$^{-O-UFM1}$ is more stable compared to
281 thioster-linked UFC1~UFM1 and therefore used for these analyses. Post preparation,

282 we incubated UFC1$^{-O-UFM1}$ with UFSP2 or 0.2N NaOH and observed complete collapse
283 only in alkaline conditions confirming that the purified UFC1$^{-O-UFM1}$ is indeed linked via
284 an oxyester linkage **(Fig S5E)**. Analysis of complex formation revealed that
285 UFL1/UFBP1 does not bind to UFC1 or UFM1 on its own but forms a stable complex
286 with UFC1$^{-O-UFM1}$ that is of high enough affinity to elute as a complex on SEC (**Fig 4E**).
287 Interestingly, even the smallest of the UFL1/UFBP1 variants was able to bind to UFC1^{-}
288 $^{O-UFM1}$ (**Fig 4F**). Taken together, the ligase complex containing the N-terminal segment
289 of UFL1 (pWH-WH1) and the C-terminal region of UFBP1(WH1'-pWH'), which we refer
290 to as UFL1/UFBP1^{min} (denoted as complex I in **Fig 4C**) is sufficient for binding to
291 charged UFC1 and may represent the minimal ligase domain sufficient to activate
292 UFC1~UFM1 for aminolysis.

293 Next, we assayed ligase activity using UFMylation assays monitoring diUFM1
294 formation. Like full length UFL1, the different C-terminal truncations co-expressed with
295 UFBP1 did not exhibit any loss of activity **(Fig 4G)**. Thus, the N-terminal region of
296 UFL1 containing (pWH-WH1) is sufficient for its ligase activity. Similarly, truncation of
297 the N-terminus region (NTR) of UFBP1 did not affect diUFM1 formation. This suggests
298 that the minimal ligase domain is sufficient to form diUFM1 chains. Lastly, we checked
299 the impact of truncations of different regions of UFL1/UFBP1 complex on their ability
300 to modify the substrates such as Histone H4 and MRE11 (**Fig 4G, S5F**). Intriguingly,
301 while deletion of regions outside of WH1, WH2 did not alter diUFM1 formation, these
302 deletions affected substrate modification. Further, deletion of the N-terminal region
303 (NTR) of UFBP1 significantly impacted substrate UFMylation suggesting roles for
304 these regions of the ligase complex in substrate recognition **(Fig 4H-I)**. Hence, using
305 systematic truncations based on AlphaFold predictions, we here make the surprising
306 discovery that three tandem WH domains **(Fig S4G)** of UFL1/UFBP1 mediate E3
307 ligase activity.

308 **CDK5RAP3 restricts the E3 ligase activity of UFL1/UFBP1**

309 Our Y2H screen identified a second hit with low significance, CDK5 regulatory subunit-
310 associated protein 3 (CDK5RAP3, also known as LZAP), an evolutionarily conserved
311 53 kDa protein that lacks any known functional domains or motifs. Secondary structure
312 analysis predicts CDK5RAP3 to contain a central unstructured region flanked by α-

313 helical stretches at the N and C terminus (**Fig S6**). To determine if CDK5RAP3 can
314 interact with UFL1 in the context of the UFL1/UFBP1 complex, we incubated
315 recombinant full length CDK5RAP3 with UFL1/UFBP1 and analysed complex
316 formation by SEC. Analysis of UV chromatograms and the fractions obtained,
317 confirmed that CDK5RAP3 interacts with UFL1/UFBP1 *in vitro* and forms a stable
318 complex (**Fig 5A**). We further analysed the complex by mass photometry which
319 confirmed the presence of a stable ternary complex with an experimental molecular
320 mass of 192 kDa (**Fig 5B**).

321 Since CDK5RAP3 forms an integral complex with UFL1/UFBP1 and CDK5RAP3 has
322 recently been suggested to function as a substrate adaptor [53], we wondered if it could
323 influence E3 ligase activity or substrate UFMylation . We therefore performed *in vitro*
324 UFMylation assays and monitored the E3 ligase activity of UFL1/UFBP1 in the
325 presence of increasing concentrations of CDK5RAP3. Surprisingly, incubation of
326 CDK5RAP3 with UFL1/UFBP1 impaired E3 ligase activity and UFMylation in a
327 concentration dependent manner **(Fig 5C)**. Moreover, preassembled
328 UFL1/UFBP1/CDK5RAP3 complexes purified by gel filtration also showed no ligase
329 activity (**Fig S7A**). These observations imply that CDK5RAP3 binds to inhibit the ligase
330 complex.

331 To gain insights into how CDK5RAP3 inhibits UFMylation, we tested if CDK5RAP3
332 inhibits complex formation between UFL1/UFBP1 and UFC1$^{-O\text{-}UFM1}$. When analysed
333 by pull down and analytical SEC, we find that CDK5RAP3 forms a complex together
334 with UFL1/UFBP1 and UFC1$^{-O\text{-}UFM1}$ (**Fig S7B-C**). Since CDK5RAP3 does not affect
335 UFC1~UFM1 binding, we next tested if CDK5RAP3 binding influences discharge of
336 UFM1 from UFC1~UFM1 by monitoring transfer of UFM1 onto free Lys. While UFM1
337 is readily discharged onto Lys in the presence of UFL1/UFBP1, this is completely
338 blocked in the presence of CDK5RAP3 (**Fig 5D-E, S7D**). These observations suggest
339 that binding of CDK5RAP3 to UFL1/UFBP1/UFC1~UFM1 complex may prevent
340 activation of UFC1~UFM1 resulting in inhibition of UFMylation.

341 While these *in vitro* experiments clearly demonstrate that CDK5RAP3 blocks UFC1
342 activation and UFMylation, it raises the question of the role of CDK5RAP3 in substrate
343 UFMylation. Therefore, we performed UFMylation assays to check for modification of

344 H4, MRE11 and TRIP4 and observed that addition of increasing concentrations of
345 CDK5RAP3 decreased UFMylation of these substrates **(Fig S7E)**. Next, we decided
346 to check the role of CDK5RAP3 in UFMylation of ribosomes, the best described
347 UFMylation substrate to date [5,6]. Hence, we set up a cell-free reconstitution of
348 ribosome UFMylation. Strikingly, addition of UFL1/UFBP1 to purified 60S ribosomes
349 leads to robust modification of RPL26 (**Fig 5F**), and in line with previous observations,
350 both mono- and di-UFMylated RPL26 are observed. When increasing concentrations
351 of CDK5RAP3 is titrated into this UFMylation reaction, the di-UFMylation of RPL26 is
352 completely abolished (**Fig 5F**). Importantly, even at the highest concentration of
353 CDK5RAP3, monoUFMylation of RPL26 is not affected. Hence, we propose
354 CDK5RAP3 to be a specificity determinant, directing activity of the ligase complex
355 towards substrate Lys by limiting spurious and off-target UFMylation.

356 **Regulation of UFC1 activity by its N-terminal helix extension**

357 In addition to its core UBC fold, UFC1 has at its N-terminus a highly conserved α-helix
358 (α0) whose function is unknown (**Fig 6A**). Moreover, UFC1 lacks the oxyanion hole
359 stabilizing Asn as part of the highly conserved HPN motif found in E2 enzymes, which
360 is instead replaced by a TAK motif at this position (**Fig 6B**). Further motivated by the
361 fact that previous studies have shown that the N- and C- terminal extensions on E2s
362 regulate E2 activity [27], we sought to determine if α0 has a role in regulating
363 UFMylation. First, we first compared the activity of $UFC1^{WT}$ and UFC1 lacking α0
364 ($UFC1^{\Delta N}$) in UFMylation assays containing UFC1 with or without UFL1/UFBP1.
365 Surprisingly, $UFC1^{\Delta N}$ showed stronger overall UFMylation compared to $UFC1^{WT}$ in the
366 presence of UFL1/UFBP1 (**Fig 6C**). This suggests an inhibitory role for the N-terminal
367 helical extension of UFC1. Next, we compared discharge of UFM1 from UFC1~UFM1
368 and $UFC1^{\Delta N}$~UFM1 onto free Lys. In the absence of E3 ligase, $UFC1^{\Delta N}$ rapidly
369 discharges UFM1 onto Lys (**Fig 6D & E**) suggesting an increase in its intrinsic lysine
370 reactivity. In the presence of UFL1/UFBP1, discharge of UFM1 onto Lys is enhanced
371 when α0 of UFC1 is deleted (**Fig 6D & F)**. Taken together with the increase in
372 UFMylation in the presence of UFL1/UFBP1, these results further cement an inhibitory
373 role for the N-terminal helix of UFC1.

374 Since we identified the N-terminal α0 of UFC1 to restrain UFMylation, we analysed if
375 inhibition by CDK5RAP3 was mediated via this helix. Indeed, UFMylation assays
376 together with discharge assays comparing activity of $UFC1^{WT}$ and $UFC1^{\Delta N}$ reveal that
377 the inhibition of E3 ligase activity by CDK5RAP3 requires the N-terminal helix of UFC1
378 (**Fig 6D & G, S8**). Based on these results we propose that CDK5RAP3 may interact
379 with both UFL1/UFBP1 and α0 of UFC1 to clamp the complex in an inhibited state.
380 Together these analyses reveal a previously unappreciated regulatory role for the N-
381 terminal helix of UFC1 in modulating UFMylation.

382

383 **Discussion**

384 In this study, we establish a robust *in vitro* reconstitution system using purified active
385 components of the UFM1 enzymatic pathway to reveal the minimal requirements for
386 UFMylation and mechanistic insights into the ligase machinery. Previous reports have
387 provided conflicting views on the roles of UFBP1 and CDK5RAP3, with some
388 suggesting that they are mainly substrates of UFMylation [13,29]. Further, it has been
389 suggested that UFBP1 must be UFMylated first at K267 before it can associate with
390 UFL1 to subsequently support UFL1 ligase activity [12]. Since both UFL1 and UFBP1
391 complexes are purified from bacteria, our work unequivocally demonstrates that UFL1
392 and UFBP1 can associate in the absence of any PTMs and the formation of this
393 complex is essential for it to function as an E3 ligase.

394 It has long been debated as to whether UFL1 is a scaffold/adaptor-type E3 ligase or a
395 Cys-based HECT-like enzyme. Scaffolding type E3 ligases such as RING E3 ligases
396 bind to both E2 and substrate to bring them together for substrate transfer. Since UFL1
397 can bind to both UFC1 and its supposed substrate UFBP1 at the same time, it was
398 suggested that UFL1 maybe a scaffold-type E3 ligase [3]. More recently, a UFMylation
399 assay that relied on UFL1 present in mammalian cell extracts to which *in vitro*
400 generated biotinylated E2~UFM1 thioesters was added, found that UFMylation
401 occurred even when cell extracts were treated with cysteine-alkylating reagents,
402 further suggesting that UFL1 could be a scaffold-type E3 ligase [13]. Our mutational
403 analysis showing that the UFL1/UFBP1 complex lacks a conserved catalytic Cys
404 combined with the ability of the E3 ligase to promote UFC1~UFM1 aminolysis
405 establish UFL1/UFBP1 as a scaffold-type E3 ligase. Further reinforcing this conclusion
406 is the observation that K69-linkage specificity is imparted by the E2 in ligase free di-
407 UFM1 formation assays and this K69-linkage specificity is maintained by the E3 ligase.
408 Indeed, this is a feature observed in RING E3 ligases where linkage-specificity is
409 determined by the E2 enzyme [31,34]. Since UFL1/UFBP1 promotes aminolysis, we
410 speculate that UFL1/UFBP1 binding induces a closed UFC1~UFM1 conformation akin
411 to RING and atypical SUMO E3 ligases [54–58].

412 UFC1 differs from prototypical E2s since it lacks the catalytic HPN motif, has an
413 exposed catalytic Cys with a lower pKa, lacks the C-terminal α-helix observed in

414 canonical E2s and has an additional α-helix at its N-terminus (α0) [25,40,59]. Further, it is
415 unclear if the canonical "backside" interaction can occur in UFC1 [28,60]. These unique
416 features of UFC1 and the unconventional features of the ligase complex makes it likely
417 that the UFM1 machinery employs a unique mechanism to transfer UFM1 from UFC1
418 onto substrate. Interestingly, the UBE2E enzymes also have an intrinsically disordered
419 N-terminal extension that have an inhibitory role restricting Ub transfer thereby limiting
420 polyUb chain formation [61]. Future work will reveal whether E3 binding induces a
421 closed UFM1~UFM1 conformation and whether α0 impedes this process.
422 Nevertheless, our data seem to suggest that α0 has a regulatory role potentially
423 preventing UFM1 discharge in the absence of the E3 ligase.

424 The recent advances in structure prediction [50] enabled us to narrow the regions of
425 UFL1/UFBP1 essential for ligase activity to a tandem repeat of three WH domains - a
426 WH domain each from UFL1 and UFBP1 and the composite WH domain formed by
427 the two proteins. As this region can bind to UFC1~UFM1 and activate the E2 for UFM1
428 discharge, we define this to be the minimal catalytic domain. Further structural studies
429 will be required to reveal why three WH domains are required to form a functional
430 ligase complex and the identification of linchpin residues in UFL1/UFBP1 that play
431 similar roles to RING E3 ligases to activate the E2 for aminolysis [55,56]. Intriguingly, the
432 anaphase promoting complex (APC) subunit APC2 contains a WHB domain that binds
433 the "backside" of UCBH10/UBE2C, located at a face opposite from the catalytic site
434 and is an allosteric site in several E2s [62,63]. This backside binding of the WHB domain
435 is specific towards UBE2C and is important for transfer of Ub onto specific substrates
436 [63]. Our observations also raise the question of the function of the other WH/PCI
437 domains in UFL1/UFBP1 to ligase function. One possibility is that the WH domains
438 may mediate substrate recognition, binding to UFM1 or serve to either regulate
439 recruitment or processivity of chain formation. Given that the WH domain of Cockayne
440 syndrome group B (CSB) can bind to ubiquitin, it is tempting to speculate that one of
441 the WH domains of UFL1/UFBP1 can bind to UFM1 [64]. WH domains commonly
442 recognize nucleic acids and are typically found in transcription factors or as protein
443 interaction domains [65]. To our knowledge, this is the first demonstration of catalytic
444 activity mediated by WH domains [66], leading us to propose moonlighting functions for
445 other WH domain containing proteins. It also raises the possibility that other WH

446 domains could have E3 ligase activity for UFMylation or other UBLs. Since UFL1 has
447 been proposed to have nuclear functions in telomere maintenance and DNA damage
448 response [10,11,67], one possibility is that the WH domains may mediate DNA binding. A
449 further possibility is the use of the WH domains of UFL1/UFBP1 to recognize rRNA or
450 translating mRNA during ribosome UFMylation.

451 Our *in vitro* studies show that formation of UFM1 chains and autoUFMylation is
452 inhibited by CDK5RAP3 (**Fig 2C**). Indeed, previous studies have observed an altered
453 pattern of UFMylation in the absence of CDK5RAP3 leading to the suggestion that it
454 may be a substrate adaptor [53]. Interestingly, CDK5RAP3 was suggested to function
455 as a sensor for ER stress to induce autophagic degradation of aberrant proteins
456 formed as a result of ribosomal stalling [68]. Several multidomain and multiprotein E3
457 ligases such as PARKIN and Cullin Ring Ligases (CRLs) are inhibited and their
458 activation is a carefully orchestrated multistep process [35,69]. Based on our
459 observations, we propose that ligase complexes containing UFL1, UFBP1 and
460 CDK5RAP3 represent an autoinhibited state. The surprising finding that ribosome
461 UFMylation is not abolished in the presence of CDK5RAP3 but rather restricted to
462 monoUFMylation leads us to suggest that CDK5RAP3 regulates ligase activity in the
463 following manner: (i) in the absence of substrate, binding of CDK5RAP3 inhibits E3
464 ligase activity; (ii) this autoinhibition is relieved when substrates such as the 60S
465 ribosome are encountered. This release from inhibition may involve conformational
466 changes induced upon recognition of structural features on the substrate by UFL1,
467 UFBP1 or CDK5RAP3 to mediate substrate UFMylation. Such multi-layered regulation
468 possibly prevents spurious UFMylation and ensures ribosome UFMylation only in the
469 right context. While previous studies have suggested roles for UFMylation for UFL1-
470 UFBP1 interaction, and UFMylation and phosphorylation to enhance UFMylation
471 [10,12,19,29], our minimal reconstitution clearly demonstrates that the ligase complex
472 assembles in the absence of any PTM. Although we cannot rule out a role for
473 phosphorylation in enhancing ligase activity, the rapid UFMylation of ribosomes by the
474 reconstituted ligase suggests that it may be unlikely.

475 Our rebuilding approach provides insights into the assembly, minimal requirements,
476 and mechanism of the UFL1/UFBP1/CDK5RAP3 ligase and reveals principles of
477 protein UFMylation. The *in vitro* reconstitution system we describe here using purified

478 components lays the foundation for future biochemical and structural studies to
479 understand the molecular mechanism of this unusual E3 ligase complex and
480 UFMylation. Further, the cell-free UFMylation system can be applied to understand
481 the logic of ribosome UFMylation and its relationship to ribosome quality control
482 pathways.

483

Acknowledgements

We thank members of the Kulathu lab for critical reading of the manuscript and helpful comments. We thank the Zeqiraj lab (Univ of Leeds) and Prof Hofmann (Univ of Köln) for helpful discussions and advice. We acknowledge MRC Reagents and Services for providing valuable reagents, especially Drs. Simone Weidlich and Rachel Toth for cloning the constructs used in this study. We thank Mr. Joby Varghese for help with Mass spectrometry data acquisition and preliminary analysis and Dr. Emma Brannigan for help with mass photometry measurements. We thank Christopher Lapointe (Puglisi lab, Stanford) for valuable reagents and discussion. We also thank Dr. Juraj Ahel (IMP Vienna) for his help with generating composite foldindex profile of UFL1. This research was supported by ERC Starting grant (RELYUBL, 677623), the Lister Institute of Preventive Medicine, BBSRC (BB/T008172/1) and MRC grant MC_UU_00018/3 to YK; Grant R01GM074874 from the National Institute of General Medical Sciences and a generous gift from the Becker Family Foundation to R.R.K; NIH Epilepsy Training Program T32 NS007280 to PAD.

Author contributions

YK and JJP conceived the study. JJP designed, performed and analysed all the experiments. HM designed, expressed and purified UFL1/UFBP1 constructs based on Alphafold. PADR performed *in vitro* ribosome UFMylation assays. DM and SPM contributed reagents and RS performed SEC MALS analysis. YK analysed data, supervised the study and secured funding. JJP and YK wrote the manuscript with input from all the authors.

Declaration of interests

The authors declare no competing interests.

Supplemental information

Supplemental information includes Figures S1-S8 and Table S1.

514

515 **Materials and Methods**

516 **Plasmids, Cloning and mutagenesis**

517 The details of cDNA constructs used in this study is given in Table S1. Cloning of most
518 of the constructs was performed by MRC PPU Reagents and Services (University of
519 Dundee). Briefly, mutagenesis was carried out using Q5 site-directed mutagenesis kit
520 (NEB) with KOD polymerase (Novagen) according to manufacturer's protocol.
521 Following mutagenesis, cDNA constructs were amplified using *E. coli* DH5α and
522 purified using QIAprep spin mini-prep kit (Qiagen). All cDNA constructs were verified
523 by DNA sequencing and services, University of Dundee using DYEnamic ET
524 terminator chemistry (Amersham Biosciences) on Applied Biosystems automated
525 DNA sequencers.

526 **Recombinant protein expression and purification**

527 Recombinant His_6-3C-UBA5, His_6-3C-UFM1^{WT}, His_6-3C-UFM1^{Konly}, His_6-3C-
528 UFM1^{KtoR}, His_6-3C-Cys-UFM1, His_6-3C-UFC1^{WT}, His6-3C-UFC1$^{\Delta N}$ and His_6-3C-
529 MRE11 were expressed in *E. coli* BL21 and purified using Ni^{2+}-NTA affinity
530 chromatography as the first step. Briefly, *E. coli* BL21 cultures expressing His_6-tagged
531 proteins were grown in 2xTY medium at 37ºC until OD_{600} reached 0.6-0.8. Final
532 concentration of 0.3 mM IPTG was added and the cultures were incubated at 18 °C
533 for 16 h. Cells were harvested, resuspended, and lysed in appropriate lysis buffer
534 containing 25 mM Tris pH 8, 300 mM NaCl, 10% Glycerol, 2 mM DTT, 1 mM
535 Benzamidine, 1 mM AEBSF, 1x protease inhibitor cocktail (Roche) by ultrasonication.
536 Lysed cells were then clarified by centrifugation at 30000g for 30 mins at 4ºC. The
537 clarified lysate was then incubated with pre-equilibrated Ni^{2+}-NTA Agarose beads
538 (Amintra, Abcam) for 2 h in appropriate binding buffer containing 25 mM Tris pH 8,
539 300 mM NaCl, 10% Glycerol,10 mM Imidazole. The beads were then washed
540 extensively using wash buffer containing 25 mM Tris pH 8, 300 mM NaCl, 10%
541 Glycerol, 2 mM DTT and 20 mM Imidazole. Finally, the bound protein was eluted using
542 elution buffer containing 25 mM Tris pH 8, 300 mM NaCl, 10% Glycerol, 2 mM DTT
543 and 300 mM Imidazole. Wherever necessary, His_6-tags were cleaved off by incubating
544 tagged proteins with PreScission protease at 4ºC overnight. A final size exclusion
545 chromatography step was performed using Superdex 75 HiLoad™ 16/60 Superdex™

546 75pg and HiLoad™ 16/60 Superdex™ 200 pg columns (GE Healthcare Life Sciences)
547 with buffer containing 25 mM Tris pH 8.0, 150 mM NaCl, 10% Glycerol and 2 mM DTT.
548 The purified proteins were then concentrated using Amicon™ Ultra 15 concentrators
549 (MERCK Millipore) and stored in -80°C.

550 **Purification of GST-tagged proteins**

551 GST-TEV-TRIP4 was expressed in *E. coli* BL21(DE3) strain as described above. Cells
552 were harvested and lysed in lysis buffer containing 25 mM Tris pH 7.5, 300 mM NaCl,
553 10% Glycerol and 2 mM DTT using ultrasonication. Pre-equilibrated Glutathione 4B-
554 sepharose beads (Amintra, abcam) were incubated with clarified lysate for 2 h. The
555 beads were then washed with high salt buffer containing 25 mM Tris pH 7.5, 500 mM
556 NaCl, 10% glycerol and 2 mM DTT. Further the beads were washed with low salt buffer
557 containing 25 mM Tris pH 8, 150 mM NaCl, 10% glycerol and 2 mM DTT. The protein
558 was then cleaved off the tag by incubation with Precision protease at 4ºC overnight. A
559 second ion exchange chromatography step was carried out using Resource Q (6ml)
560 (GE Healthcare Life Sciences) column with low salt buffer as 25mM Tris pH 7.5, 150
561 mM NaCl, 10% glycerol, 2 mM DTT and high salt buffer as 25mM Tris pH 7.5, 500mM
562 NaCl, 10% glycerol and 2 mM DTT. A final size exclusion chromatography step was
563 performed using HiLoad™ 16/60 Superdex™ 75pg (GE Healthcare Life Sciences) and
564 the protein was buffer exchanged in buffer 25 mM Tris pH 7.5, 150 mM NaCl, 10%
565 glycerol and 2 mM DTT. The purified proteins were then concentrated and stored in -
566 80ºC.

567 **Co-expression and purification of UFL1-UFBP1 complex**

568 His_6-TEV-UFL1 and StrepII-C3-UFBP1 were cloned in a pET Duet1 construct and
569 expressed in *E. coli* BL21 codon plus (RIPL) (Agilent) cells. Bacterial cultures were
570 grown in 2xTY medium at 37°C until OD_{600} reached 0.6. Final concentration of 0.3 mM
571 IPTG was added to induce the expression and the cultures were incubated at 18°C for
572 16 h. Cells were harvested, resuspended in buffer containing 25 mM Tris pH 8.0, 300
573 mM NaCl, 2 mM DTT, 1mM Benzamidine, 1mM AEBSF, protease inhibitor cocktails
574 (Roche). Cells were lysed by High pressure homogenization using French press
575 (Avestin Emulsiflux C3, Wolflabs). The lysate was then clarified by Ultracentrifugation
576 at 30000g for 30 mins at 4°C. Affinity purification was carried out in two steps. In the
577 first step, the clarified lysate (25 mM Tris pH 8.0, 300 mM NaCl, 20 mM Imidazole, 2

578 mM DTT) was passed through HisTrap™ FF (GE Healthcare Life Sciences) column.
579 After binding, the column was washed with 10 column volumes (CV) of binding buffer
580 containing 25 mM Tris pH 8.0, 300 mM NaCl, 20 mM Imidazole, 2 mM DTT. After
581 washing, bound proteins were eluted using buffer containing 25 mM Tris pH 8.0, 300
582 mM NaCl, 300 mM Imidazole, 2 mM DTT by applying a concentration gradient of
583 Imidazole. The eluted proteins were then passed through StrepTrap™ (GE Healthcare
584 Life Sciences) column pre-equilibrated with buffer containing 25 mM Tris pH 8.0, 300
585 mM NaCl, 2 mM DTT. After 2 CV of washing with binding buffer, the proteins were
586 eluted using 25 mM Tris pH 8.0, 300 mM NaCl, 2 mM DTT and 2.5 mM Desthiobiotin.
587 Finally, purified proteins were passed through HiLoad™ 16/60 Superdex™ 200pg (GE
588 Healthcare Life Sciences). The purified protein was then stored in -80°C in buffer
589 containing 25 mM Tris pH 8.0, 300 mM NaCl, 5% Glycerol and 2 mM DTT until further
590 use.

591 **Preparation and labelling of IRDye800CW-UFM1**

592 Cys-UFM1$^{1-83}$ which contains a Cys residue upstream of M1 was purified and
593 exchanged into a fresh buffer containing 50 mM HEPES pH 7.5, 150 mM NaCl and
594 0.5 mM TCEP using CentriPure P10 columns (EMP Biotech). Protein was then mixed
595 with IRDye® 800CW Maleimide (LI-COR®) at 5:1 molar ratio and incubated for 2 h at
596 RT. Unreacted dye was removed by three-step buffer exchange process using
597 CentriPure P10 columns (EMP Biotech) (once) and PD-10 Sephadex G-25 column
598 (twice) in a sequential manner according to manufacturer's instruction. Finally, to
599 remove residual unreacted dye material, the labelled protein was dialyzed into buffer
600 containing 25 mM Tris pH 8, 150 mM NaCl and 2 mM DTT using dialysis membrane
601 (Thermo Scientific) (MWCO 3000) overnight at 4°C and stored at -80°C until further
602 use.

603 **Biochemical assays**

604 **Lysine discharge assays**

605 To analyse the intrinsic reactivity of UFC1, a substrate-independent single turnover
606 discharge assay was employed. Firstly, UFC1 was charged with UFM1^{WT} or labelled
607 UFM1 by incubating 0.5 μM UBA5, 10 μM UFC1 and 20 μM UFM1 in a buffer
608 containing 50 mM HEPES pH 7.5, 50 mM NaCl, 0.5 mM DTT and10 mM $MgCl_2$. The

609 charging reaction was initiated by addition of 10 mM ATP and incubation of the
610 reaction mix at 37°C for 20-30 mins. To stop further charging of UFM1 onto UFC1, the
611 reaction was quenched by addition of 50 mM EDTA and subsequent incubation at RT
612 for 10 mins. To check for discharge, the quenched mixture was incubated with 50 mM
613 lysine (pH 8.0) or other amino acids namely Serine, Threonine, Arginine, Cysteine at
614 37°C. The reaction was stopped at each of the time points by addition of SDS-Loading
615 dye without any reducing agent to the reaction mix and run on a 4-12% SDS-PAGE
616 under non-reducing conditions followed by Coomassie staining or visualization using
617 LI-COR® Odyssey.
618 In reactions involving the UBE2D3 and UBE2L3, 0.5 μM UBE1 was incubated with 10
619 μM UBE2D3/UBE2L3 and 20 μM Ub in reaction buffer containing 50 mM HEPES pH
620 7.5, 50 mM NaCl,10 mM ATP and 10 mM $MgCl_2$ at 37°C for 20 mins. The reaction
621 was quenched, and discharge was analysed as described above.
622 In discharge assays involving UFL1/UFBP1 and CDK5RAP3, the quenched reaction
623 mix was added to a cocktail containing 1 µM UFL1/UFBP1 or 1 μM or 2 μM of
624 CDK5RAP3. Discharge was initiated by addition of 50 mM lysine (pH 8.0) in buffer
625 containing 50 mM HEPES pH 7.5, 50 mM NaCl and 0.5 mM DTT and incubated at
626 37°C for indicated time duration. The reaction was stopped and analysed as described
627 above.

628 ***In vitro* UFMylation assays**

629 To check for UFMylation *in vitro,* 0.25 μM UBA5, 5 µM UFC1, 1 µM UFL1 and 20-30
630 µM UFM1 were incubated in reaction buffer containing 50 mM HEPES 7.5, 10 mM
631 $MgCl_2$ and 5 mM ATP for 1 h at 37ºC. The reaction was stopped by the addition of
632 SDS loading buffer containing a reducing agent. The reaction products were then
633 separated on a 4-12% SDS-PAGE gel under reducing conditions and analysed by
634 immunoblotting using indicated antibodies. In UFMylation assays involving substrates,
635 around 1 µM-2 µM of recombinant substrates were incubated with 0.25 µM UBA5, 5
636 µM UFC1, 1µM UFL1 and 30 µM of UFM1 in buffer containing 50 mM HEPES 7.5,10
637 mM $MgCl_2$ and 5 mM ATP for 1 h at 37°C. Following incubation, the reaction was
638 stopped and analyzed using SDS-PAGE or Immunoblotting using indicated
639 antibodies.

640 **Pulldown assays**

641 To analyse the interaction of the E3 ligase with the E2, pulldown assays were
642 performed. Approximately 10 μM of untagged UFC1 or UFC1$^{-O-UFM1}$ was incubated
643 with 5 μM of full length UFL1/UFBP1 in binding buffer containing 25 mM Tris pH 8.0,
644 300 mM NaCl, 2 mM DTT for 1 h at 4°C. Following incubation, 30 μl of pre-equilibrated
645 Streptavidin Sepharose beads (IBA Life Sciences) (50% slurry) was added and further
646 incubated for about 1h at 4°C. Following binding, centrifuge tubes containing the
647 reaction mix was spun down at 500g for 3 mins and the supernatant was discarded to
648 remove unbound proteins. To further remove weakly bound proteins, the beads were
649 washed thrice with 1 ml of ice-cold binding buffer. Finally, the bound proteins were
650 eluted by addition of binding buffer containing 2.5 mM Desthiobiotin (pH 8.0) and
651 incubation at 4°C for 30 min. The eluates were then analysed on 4-12% SDS PAGE
652 under reducing conditions followed by Coomassie staining.

653 **Analytical gel filtration chromatography analysis**

654 For analysing the interaction between UFL1/UFBP1 and CDK5RAP3, around 30 μg of
655 UFL1/UFBP1 and 15 μg of CDK5RAP3 were mixed and incubated for 30 min on ice.
656 Then, around 50 μls of sample was loaded on Superdex^{TM} 200 Increase 3.2/300
657 column (GE Healthcare Lifesciences) pre-equilibrated with buffer containing 25 mM
658 Tris pH 8.0, 300 mM NaCl and 2 mM DTT. The fractions corresponding to each peak
659 were collected and further analysed on a 4-12% SDS PAGE under reducing conditions
660 followed by Coomassie staining.

661 To check if UFL1/ UFBP1 could be reconstituted *in trans*, around 15 μg of purified
662 His$_6$-UFL1 and StrepII-UFBP1 were mixed and incubated on ice for 2h. After
663 incubation, sample was loaded on Superdex^{TM} 200 Increase 3.2/300 column (GE
664 Healthcare Lifesciences) column pre-equilibrated with buffer containing 25 mM Tris
665 pH 8.0, 300 mM NaCl, 2 mM DTT and the chromatograms were analysed.

666 **Preparation of UFC1$^{-O-UFM1}$**

667 UFC1$^{-O-UFM1}$ was prepared by incubating 40 μM UFC1^{C116S} with 40 μM UFM1, 1 μM
668 UBA5 in buffer containing 50 mM Tris pH 8.8, 10 mM $MgCl_2$, 5 mM ATP overnight at
669 25°C. The reaction was incubated briefly with 20 mM DTT to remove any non-specific
670 di-sulfide linked adducts formed and passed through HiLoad^{TM} 16/60 Superdex^{TM} 75
671 pg with buffer containing 25 mM Tris pH 8.0, 150 mM NaCl, 5% Glycerol and 2 mM

672 DTT. The fractions corresponding to UFC1$^{-O-UFM1}$ were collected and analysed on 4-
673 12% SDS PAGE gel. Finally, the fractions containing UFC1$^{-O-UFM1}$ were pooled,
674 concentrated and stored in -80°C until further use.

675 **Alphafold Predictions**

676 The structure of UFL1/UFBP1 was predicted using the ColabFold Google Colab
677 notebook "AlphaFold_advanced" [50] (https://github.com/sokrypton/ColabFold). The
678 predicted model with the highest IDDT score is shown in the main figure and the PAE
679 scores for different models ranking 1 to 5 are shown in **Fig S4A**.

680 **DALI Analysis**

681 DALI server was used to perform structural similarity analysis [70]. WH1 domain of
682 UFL1(52-115) was used as the query model and searched against PDB25 database.
683 The top ten models in the order of the Z-score is shown in **Fig S4B**.

684 **Bioinformatic analysis**

685 For generation of composite Foldindex profile, previously reported method was
686 adapted [71,72]. First, individual Foldindex profiles of UFL1 sequence from different
687 organisms were generated locally using a custom foldindex program provided by Juraj
688 Ahel. Then, a composite Foldindex profile was prepared by blending the images in
689 Adobe illustrator with 30% opacity.
690 For generation of multiple sequence aligments, the protein sequences of target
691 proteins and their homologs were manually downloaded from UNIPROT database in
692 fasta format. Multiple sequence alignment was performed using Jalview version
693 2.11.1.7 programme (MAFFT algorithm module using L-INS-I) [73,74].

694 **Mass Photometry Data Acquisition and Analysis**

695 Protein samples were prepared in a solution containing 25 mM Tris pH 8.0, 300 mM
696 NaCl, 2 mM DTT and stored on ice before loading onto the Refeyn One^{MP} instrument
697 (Refeyn). Typically, a set of protein standards (NativeMark™ Unstained Protein
698 Standard, Invitrogen) are used for calibration and to generate a standard curve.
699 Following calibration, approximately 10 μl of diluted protein sample in the
700 concentration range of 5–25 nM was introduced into the flow-chamber and movies of
701 60s duration were recorded. Data acquisition was performed using Acquire MP

702 (Refeyn Ltd, v1.1.3) and analysed using Discover MP software. Data shown here is
703 representation of at least 3 independent acquisitions ($n \geq 3$).

704 **SEC MALS data acquisition and analysis**

705 Size exclusion chromatography and multi angle light scattering (SEC–MALS)
706 experiments were performed on a Dionex Ultimate 3000 HPLC system with an inline
707 Wyatt miniDAWN TREOS MALS detector and Optilab T-rEX refractive index detector.
708 In addition, the elution profile of the protein was monitored with UV 280 attached to
709 the Dionex system. For size exclusion chromatography, Superdex 200 10/300 gl
710 column (GE Healthcare LifeSciences) was used. 50 μl of the purified UFL1/UFBP1
711 stored in buffer containing 25 mM Tris pH 8.0, 300 mM NaCl, 2 mM DTT was loaded
712 into the SEC column with Dionex auto loader at a concentration of 4 mg/ml and a flow
713 rate of 0.3 ml/min was maintained throughout the experiment. Molar masses spanning
714 elution peaks were calculated using ASTRA v6.0.0.108 (Wyatt).

715 **Ribosome UFMylation assays**

716 Purified 60S ribosomes were a generous gift from the Puglisi lab, and purified as
717 described previously [75,76]. *In vitro* UFMylation of ribosomes was performed at 30 ºC
718 with 1 μM UFC1, 0.5 μM UBA5, 0.5 μM UFM1, 0 nM or 75 nM UFL1/UFBP1, 50 nM
719 purified 60S ribosomes, and increasing concentrations of CDK5RAP3 (0, 38, 75, 150
720 or 375 nM) in a reaction buffer of 25 mM HEPES pH 7.5, and 100 mM NaCl. The
721 reaction was quenched in 4 x SDS-Load buffer. Western blots show 10 min reaction
722 time; immunoblots for RPL26 (Abcam, 59567) and UFL1 (Bethyl, A303-455M) were
723 run on the same gel, which was cut and probed for these proteins separately.
724 Immunoblots for CDK5RAP3 Bethyl, A300-871A) and UFM1 (Abcam, Ab109307)
725 were run on separate gels.

726 **LC-MS/MS sample preparation, data acquisition and analysis**

727 First, an *in vitro* UFMylation reaction was performed to generate UFMylated products
728 including free UFM1 chains. Then, the reaction products were run on a 4-12% SDS
729 PAGE gel to separate the products based on electrophoretic mobility. Next, the bands
730 corresponding to di-UFM1 chains were excised and in-gel digestion was performed [77].
731 Digested peptides were analysed by LC-MS/MS on an Exploris 480 coupled to an
732 Ultimate 3000 nanoLC system (Thermo Fisher Scientific) for figure 2D and on an

733 Exploris 240 (Thermo Fisher Scientific) coupled to an Evosep One (Evosep) for figure
734 4D. For the analysis performed on the Ultimate 3000, samples were loaded on a 100
735 μm x 2 cm trap column (Thermo Fisher Scientific #164564-CMD) and analysed on a
736 75 μm x 50 cm analytical column (Thermo Fisher Scientific #ES903) using a gradient
737 from 3% to 35% Buffer B (80% LCMS grade acetonitrile, 0.08% formic acid in water)
738 over 53 minutes. The columns were then washed with 95% Buffer B for 2 minutes prior
739 equilibration in 97% Buffer A (0.1% formic acid in LCMS grade water). For the analysis
740 performed on the Evosep One, samples were loaded onto the Evotips as per
741 manufacturer recommendations and analysed using the 30 SPD Method. Peptides
742 were then analysed in on either the Exploris 240 or 480 using data dependant with a
743 MS1 resolution of 60000, AGC target of 300% and maximum injection time of 25 or
744 28 ms. Peptide were then fragmented using TOP 2 s method, MS2 resolution of
745 15000, NCE of 30 or 32%, AGC of 100% and maximum injection time of 100 ms.
746 Peptide identification was performed in Mascot using a restricted and frequently
747 updated database containing ~2000 protein sequences of interest (MRC db).
748 Carbamidomethylation (C) was set at fixed modification and Oxidation (M), Dioxidation
749 (M) and the addition of the dipeptide Glycine-Valine (K) were set as variable
750 modifications. Peptides were searched using an MS1 tolerance of 10 ppm and MS2
751 tolerance of 0.06 Da and a maximum of 2 missed cleavages were allowed. Only hits
752 identified with a FDR (False Discovery Rate) <1% were selected and further analysed
753 in Scaffold viewer V5. For semi-quantitative analysis of VG modification on individual
754 sites, Total Ion chromatogram (TIC) values obtained from the LC/MS and represented
755 graphically.
756
757

758 **References:**

759 1. Van Der Veen, A. G. & Ploegh, H. L. Ubiquitin-like proteins. *Annu. Rev. Biochem.* **81**,
760 323–357 (2012).
761 2. Sasakawa, H. *et al.* Solution structure and dynamics of Ufm1, a ubiquitin-fold modifier
762 1. *Biochem. Biophys. Res. Commun.* **343**, (2006).
763 3. Komatsu, M. *et al.* A novel protein-conjugating system for Ufm1, a ubiquitin-fold
764 modifier. *EMBO J.* **23**, 1977–1986 (2004).
765 4. Cappadocia, L. & Lima, C. D. Ubiquitin-like Protein Conjugation: Structures,
766 Chemistry, and Mechanism. *Chemical Reviews* vol. 118 889–918 (2018).
767 5. Walczak, C. P. *et al.* Ribosomal protein RPL26 is the principal target of UFMylation.
768 *Proc. Natl. Acad. Sci. U. S. A.* **116**, 1299–1308 (2019).
769 6. Wang, L. *et al.* UFMylation of RPL26 links translocation-associated quality control to
770 endoplasmic reticulum protein homeostasis. *Cell Res.* **30**, 5–20 (2020).
771 7. Liang, J. R. *et al.* A Genome-wide ER-phagy Screen Highlights Key Roles of
772 Mitochondrial Metabolism and ER-Resident UFMylation. *Cell* **180**, 1160-1177.e20
773 (2020).
774 8. Wang, Z. *et al.* MRE11 UFMylation promotes ATM activation. *Nucleic Acids Res.* **47**,
775 (2019).
776 9. Liu, J. *et al.* UFMylation maintains tumour suppressor p53 stability by antagonizing its
777 ubiquitination. *Nat. Cell Biol.* **22**, 1056–1063 (2020).
778 10. Qin, B. *et al.* UFL1 promotes histone H4 ufmylation and ATM activation. *Nat.*
779 *Commun.* **10**, (2019).
780 11. Lee, L. *et al.* UFMylation of MRE11 is essential for maintenance of telomere length
781 and hematopoietic stem cell survival. (2019) doi:10.1101/846477.
782 12. Yoo, H. M. *et al.* Modification of asc1 by ufm1 is crucial for erα transactivation and
783 breast cancer development. *Mol. Cell* **56**, 261–274 (2014).
784 13. Gak, I. A. *et al.* UFMylation regulates translational homeostasis and cell cycle
785 progression. *bioRxiv* (2020) doi:10.1101/2020.02.03.931196.
786 14. Xie, Z., Fang, Z. & Pan, Z. Ufl1/RCAD, a Ufm1 E3 ligase, has an intricate connection
787 with ER stress. *International Journal of Biological Macromolecules* vol. 135 760–767
788 (2019).
789 15. Liu, J. *et al.* A critical role of DDRGK1 in endoplasmic reticulum homoeostasis via
790 regulation of IRE1α stability. *Nat. Commun.* **8**, (2017).
791 16. Duan, R. *et al.* UBA5 mutations cause a new form of autosomal recessive cerebellar
792 ataxia. *PLoS One* **11**, 1–12 (2016).
793 17. Nahorski, M. S. *et al.* Biallelic UFM1 and UFC1 mutations expand the essential role of
794 ufmylation in brain development. *Brain* **141**, 1934–1945 (2018).
795 18. Tatsumi, K. *et al.* The Ufm1-activating enzyme Uba5 is indispensable for erythroid
796 differentiation in mice. *Nat. Commun.* **2**, (2011).
797 19. Lemaire, K. *et al.* Ubiquitin fold modifier 1 (UFM1) and its target UFBP1 protect
798 pancreatic beta cells from ER stress-induced apoptosis. *PLoS One* **6**, (2011).
799 20. Cai, Y. *et al.* UFBP1, a Key Component of the Ufm1 Conjugation System, Is Essential
800 for Ufmylation-Mediated Regulation of Erythroid Development. *PLoS Genet.* **11**,
801 (2015).
802 21. Cai, Y., Singh, N. & Li, H. Essential role of Ufm1 conjugation in the hematopoietic
803 system. *Experimental Hematology* vol. 44 (2016).
804 22. Sung, H. K. *et al.* Two novel ubiquitin-fold modifier 1 (Ufm1)-specific proteases,
805 UfSP1 and UfSP2. *J. Biol. Chem.* **282**, 5256–5262 (2007).
806 23. Oweis, W. *et al.* Trans-Binding Mechanism of Ubiquitin-like Protein Activation
807 Revealed by a UBA5-UFM1 Complex. *Cell Rep.* **16**, 3113–3120 (2016).

24. Banerjee, S., Kumar, M. & Wiener, R. Decrypting UFMylation: How proteins are modified with UFM1. *Biomolecules* **10**, 1–14 (2020).
25. Mizushima, T. *et al.* Crystal structure of Ufc1, the Ufm1-conjugating enzyme. *Biochem. Biophys. Res. Commun.* **362**, 1079–1084 (2007).
26. Liu, G. *et al.* NMR and X-RAY structures of human E2-like ubiquitin-fold modifier conjugating enzyme 1 (UFC1) reveal structural and functional conservation in the metazoan UFM1-UBA5-UFC1 ubiquination pathway. *J. Struct. Funct. Genomics* **10**, 127–136 (2009).
27. Stewart, M. D., Ritterhoff, T., Klevit, R. E. & Brzovic, P. S. E2 enzymes: More than just middle men. *Cell Res.* **26**, 423–440 (2016).
28. Brzovic, P. S., Lissounov, A., Christensen, D. E., Hoyt, D. W. & Klevit, R. E. A UbcH5/ubiquitin noncovalent complex is required for processive BRCA1-directed ubiquitination. *Mol. Cell* **21**, 873–880 (2006).
29. Tatsumi, K. *et al.* A novel type of E3 ligase for the Ufm1 conjugation system. *J. Biol. Chem.* **285**, 5417–5427 (2010).
30. Cai, Y. *et al.* Indispensable role of the Ubiquitin-fold modifier 1-specific E3 ligase in maintaining intestinal homeostasis and controlling gut inflammation. *Cell Discov.* **5**, (2019).
31. Deol, K. K., Lorenz, S. & Strieter, E. R. Enzymatic Logic of Ubiquitin Chain Assembly. *Front. Physiol.* **10**, 1–14 (2019).
32. Pichler, A., Fatouros, C., Lee, H. & Eisenhardt, N. SUMO conjugation - A mechanistic view. *Biomolecular Concepts* vol. 8 13–36 (2017).
33. Lorenz, S. Structural mechanisms of HECT-type ubiquitin ligases. *Biol. Chem.* **399**, 127–145 (2018).
34. Deshaies, R. J. & Joazeiro, C. A. P. RING domain E3 ubiquitin ligases. *Annu. Rev. Biochem.* **78**, 399–434 (2009).
35. Walden, H. & Rittinger, K. RBR ligase–mediated ubiquitin transfer: a tale with many twists and turns. *Nat. Struct. Mol. Biol.* **25**, 440–445 (2018).
36. Pao, K. *et al.* Ligase With Esterification Activity. *Nature* (2018).
37. Wu, J., Lei, G., Mei, M., Tang, Y. & Li, H. A novel C53/LZAP-interacting protein regulates stability of C53/LZAP and DDRGK domain-containing protein 1 (DDRGK1) and modulates NF-κB signaling. *J. Biol. Chem.* **285**, 15126–15136 (2010).
38. Witting, K. F. & Mulder, M. P. C. Highly specialized ubiquitin-like modifications: Shedding light into the ufm1 enigma. *Biomolecules* vol. 11 (2021).
39. Gerakis, Y., Quintero, M., Li, H. & Hetz, C. The UFMylation System in Proteostasis and Beyond. *Trends in Cell Biology* vol. 29 (2019).
40. Kumar, M. *et al.* Structural basis for UFM1 transfer from UBA5 to UFC1. *Nat. Commun.* **12**, (2021).
41. Padala, P. *et al.* Novel insights into the interaction of UBA5 with UFM1 via a UFM1-interacting sequence. *Sci. Rep.* **7**, 1–12 (2017).
42. Soudah, N. *et al.* An N-Terminal Extension to UBA5 Adenylation Domain Boosts UFM1 Activation: Isoform-Specific Differences in Ubiquitin-like Protein Activation. *J. Mol. Biol.* **431**, 463–478 (2019).
43. Wenzel, D. M., Lissounov, A., Brzovic, P. S. & Klevit, R. E. UBCH7 reactivity profile reveals parkin and HHARI to be RING/HECT hybrids. *Nature* **474**, 105–108 (2011).
44. Kihm, A. J. *et al.* An abundant erythroid protein that stabilizes free α-haemoglobin. *Nature* **417**, 758–763 (2002).
45. Warner, J. R. In the absence of ribosomal RNA synthesis, the ribosomal proteins of HeLa Cells are synthesized normally and degraded rapidly. *J. Mol. Biol.* **115**, 315–333 (1977).
46. Yanagitani, K., Juszkiewicz, S. & Hegde, R. S. UBE2O is a quality control factor for

859 orphans of multiprotein complexes. *Science (80-.).* **357**, 472–475 (2017).
860 47. Sonn-Segev, A. *et al.* Quantifying the heterogeneity of macromolecular machines by
861 mass photometry. *Nat. Commun.* **11**, 1–10 (2020).
862 48. Deng, L. *et al. Activation of the IB Kinase Complex by TRAF6 Requires a Dimeric*
863 *Ubiquitin-Conjugating Enzyme Complex and a Unique Polyubiquitin Chain through*
864 *covalent modification by Ub*. *Cell* vol. 103 (2000).
865 49. Branigan, E., Plechanovová, A., Jaffray, E. G., Naismith, J. H. & Hay, R. T. Structural
866 basis for the RING-catalyzed synthesis of K63-linked ubiquitin chains. *Nat. Struct.*
867 *Mol. Biol.* **22**, 597–602 (2015).
868 50. Jumper, J. *et al.* Highly accurate protein structure prediction with AlphaFold. *Nature*
869 **596**, 583–589 (2021).
870 51. Stewart, M. Structural biology of the PCI-protein fold. *Bioarchitecture* vol. 2 118–123
871 (2012).
872 52. Scheel, H. & Hofmann, K. Prediction of a common structural scaffold for proteasome
873 lid, COP9-signalosome and eIF3 complexes. *BMC Bioinformatics* **6**, (2005).
874 53. Yang, R. *et al.* CDK5RAP3, a UFL1 substrate adaptor, is crucial for liver development.
875 *Dev.* **146**, (2019).
876 54. Pichler, A., Knipscheer, P., Saitoh, H., Sixma, T. K. & Melchior, F. The RanBP2
877 SUMO E3 ligase is neither HECT- nor RING-type. *Nat. Struct. Mol. Biol.* **11**, 984–991
878 (2004).
879 55. Plechanovov, A., Jaffray, E. G., Tatham, M. H., Naismith, J. H. & Hay, R. T. Structure
880 of a RING E3 ligase and ubiquitin-loaded E2 primed for catalysis. *Nature* **489**, 115–
881 120 (2012).
882 56. Pruneda, J. N. *et al.* Structure of an E3:E2~Ub Complex Reveals an Allosteric
883 Mechanism Shared among RING/U-box Ligases. *Mol. Cell* **47**, 933–942 (2012).
884 57. Reverter, D. & Lima, C. D. Insights into E3 ligase activity revealed by a SUMO–
885 RanGAP1–Ubc9–Nup358 complex. *Nature* **435**, 687–692 (2005).
886 58. Cappadocia, L., Pichler, A. & Lima, C. D. Structural basis for catalytic activation by the
887 human ZNF451 SUMO E3 ligase. *Nat. Struct. Mol. Biol.* **22**, 968–975 (2015).
888 59. Gundogdu, M. & Walden, H. Structural basis of generic versus specific E2–RING E3
889 interactions in protein ubiquitination. *Protein Sci.* **28**, 1758–1770 (2019).
890 60. Middleton, A. J., Wright, J. D. & Day, C. L. Regulation of E2s: A Role for Additional
891 Ubiquitin Binding Sites? *J. Mol. Biol.* **429**, 3430–3440 (2017).
892 61. Schumacher, F.-R., Wilson, G. & Day, C. L. The N-Terminal Extension of UBE2E
893 Ubiquitin-Conjugating Enzymes Limits Chain Assembly. *J. Mol. Biol.* **425**, 4099–4111
894 (2013).
895 62. Brzovic, P. S. *et al.* Binding and recognition in the assembly of an active
896 BRCA1/BARD1 ubiquitin-ligase complex. *Proc. Natl. Acad. Sci. U. S. A.* **100**, 5646–
897 5651 (2003).
898 63. Brown, N. G. *et al.* RING E3 mechanism for ubiquitin ligation to a disordered substrate
899 visualized for human anaphase-promoting complex. *Proc. Natl. Acad. Sci.* **112**, 5272–
900 5279 (2015).
901 64. Takahashi, T. S. *et al.* Structural basis of ubiquitin recognition by the winged-helix
902 domain of Cockayne syndrome group B protein. *Nucleic Acids Res.* **47**, 3784–3794
903 (2019).
904 65. Harami, G. M., Gyimesi, M. & Kovács, M. From keys to bulldozers: Expanding roles
905 for winged helix domains in nucleic-acid-binding proteins. *Trends in Biochemical*
906 *Sciences* vol. 38 364–371 (2013).
907 66. ARAVIND, L., ANANTHARAMAN, V., BALAJI, S., BABU, M. & IYER, L. The many
908 faces of the helix-turn-helix domain: Transcription regulation and beyond. *FEMS*
909 *Microbiol. Rev.* **29**, 231–262 (2005).

910 67. Qin, B. *et al.* STK38 promotes ATM activation by acting as a reader of histone H4
911 ufmylation. *Sci. Adv.* **6**, 1–10 (2020).
912 68. Stephani, M. *et al.* A cross-kingdom conserved er-phagy receptor maintains
913 endoplasmic reticulum homeostasis during stress. *Elife* **9**, (2020).
914 69. Baek, K., Scott, D. C. & Schulman, B. A. NEDD8 and ubiquitin ligation by cullin-RING
915 E3 ligases. *Curr. Opin. Struct. Biol.* **67**, 101–109 (2021).
916 70. Holm, L. Using Dali for Protein Structure Comparison. in 29–42 (2020).
917 doi:10.1007/978-1-0716-0270-6_3.
918 71. Ahel, J. *et al.* Moyamoya disease factor RNF213 is a giant E3 ligase with a dynein-like
919 core and a distinct ubiquitin-transfer mechanism. *Elife* **9**, 1–23 (2020).
920 72. Prilusky, J. *et al.* FoldIndex(C): a simple tool to predict whether a given protein
921 sequence is intrinsically unfolded. *Bioinformatics* **21**, 3435–3438 (2005).
922 73. Waterhouse, A. M., Procter, J. B., Martin, D. M. A., Clamp, M. & Barton, G. J. Jalview
923 Version 2--a multiple sequence alignment editor and analysis workbench.
924 *Bioinformatics* **25**, 1189–1191 (2009).
925 74. Katoh, K. & Toh, H. Parallelization of the MAFFT multiple sequence alignment
926 program. *Bioinformatics* **26**, 1899–1900 (2010).
927 75. Johnson, A. G. *et al.* RACK1 on and off the ribosome. *RNA* **25**, 881–895 (2019).
928 76. Lapointe, C. P. *et al.* Dynamic competition between SARS-CoV-2 NSP1 and mRNA
929 on the human ribosome inhibits translation initiation. *Proc. Natl. Acad. Sci.* **118**,
930 e2017715118 (2021).
931 77. Shevchenko, A., Tomas, H., Havliš, J., Olsen, J. V. & Mann, M. In-gel digestion for
932 mass spectrometric characterization of proteins and proteomes. *Nat. Protoc.* **1**, 2856–
933 2860 (2007).
934

935 **Figures**

936

Figure 1

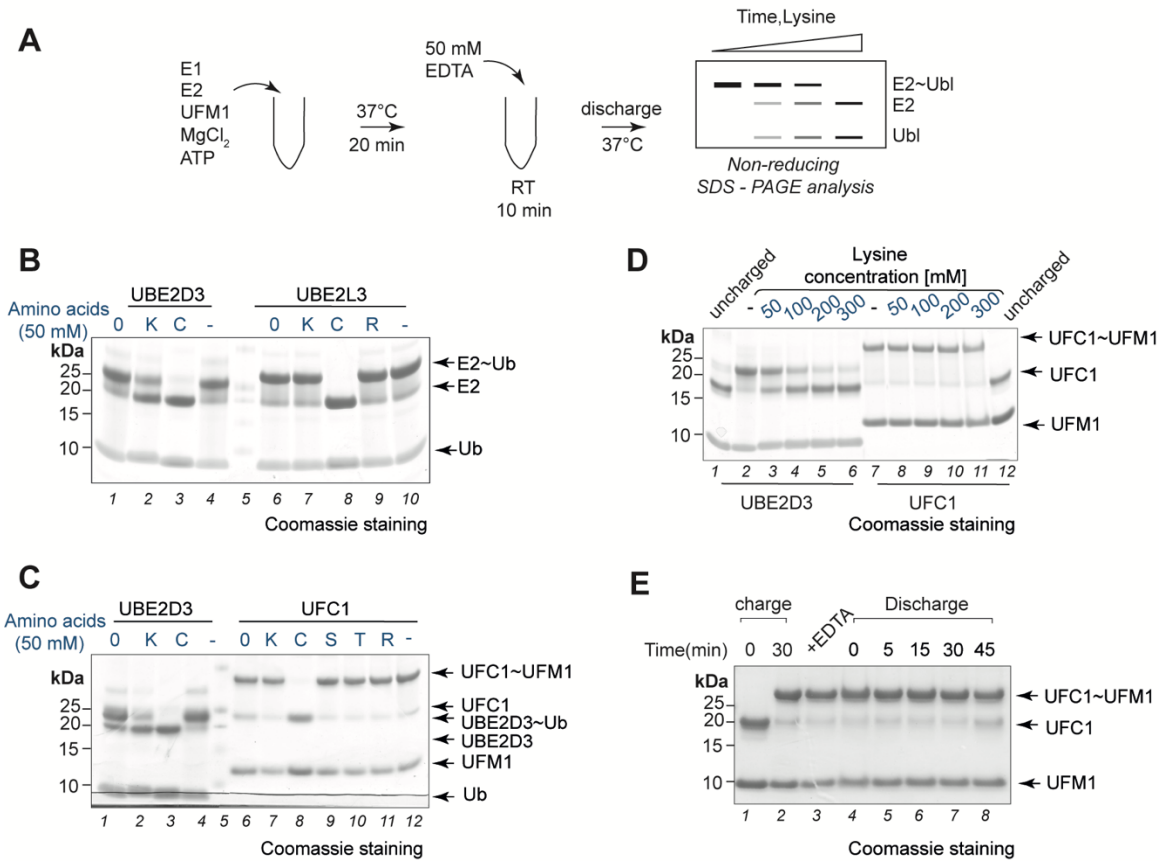

937

938 **Figure 1: - Nucleophilic reactivity profiling of UFC1**

939 **A.** Schematic showing the workflow for substrate independent single turnover
940 lysine discharge assays.

941 **B.** Assay to monitor discharge of Ubiquitin from UBE2D3 and UBE2L3 in the
942 presence of free amino acids. 0 indicates time 0.

943 **C.** Assay to check for discharge of UFM1 from UFC1 in the presence of free amino
944 acids. UBE2D3 is used as a positive control for lysine and cysteine discharge.

945 **D.** Lysine discharge assays using UBE2D3 and UFC1 in the presence of
946 increasing concentration of free Lysine.

947 **E.** Time-dependent analysis of discharge of UFM1 from UFC1 in the presence of
948 high concentration of free lysine (150 mM).

949

950

Figure 2

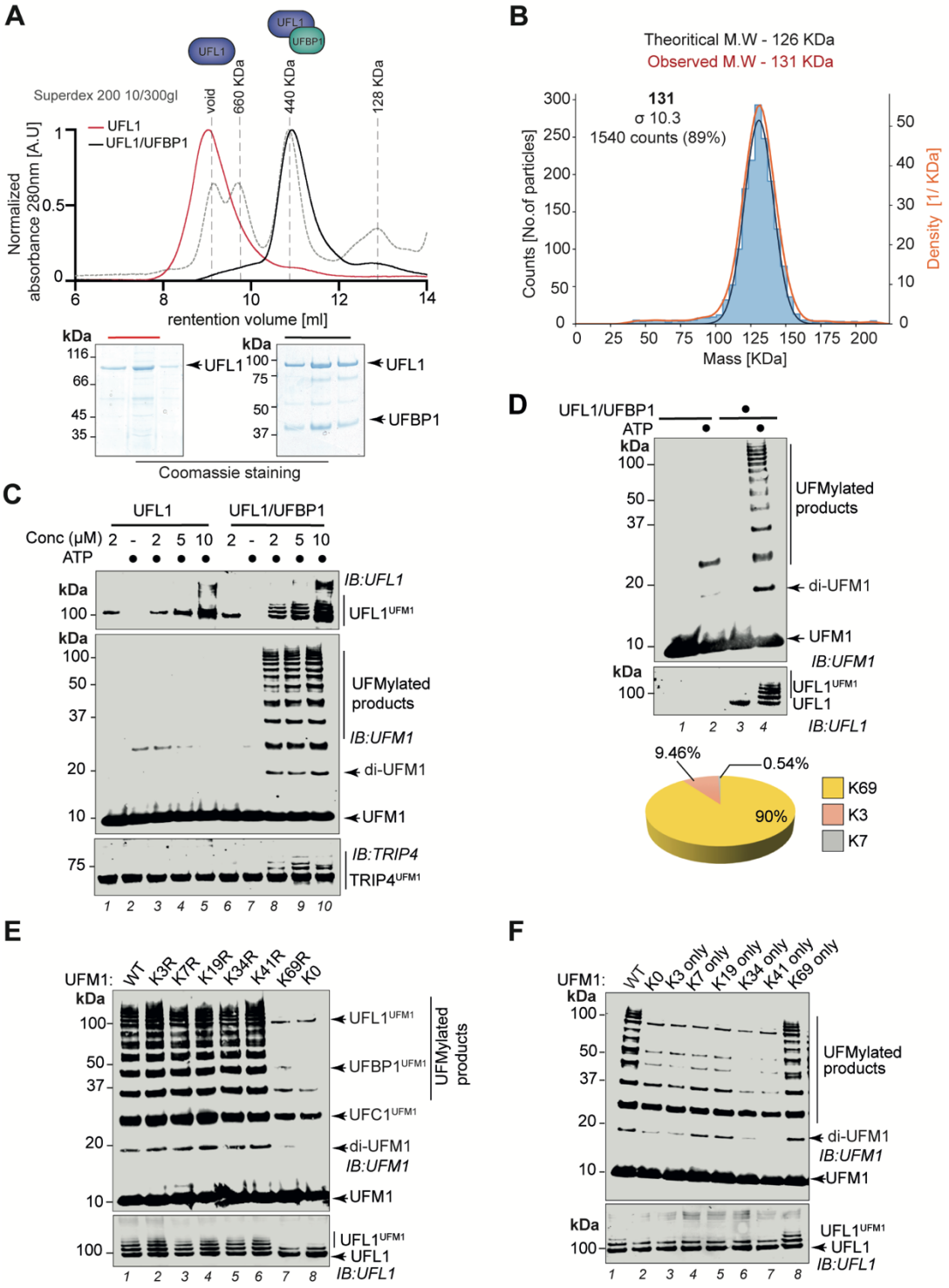

Figure 2: - *In vitro* reconstitution of the active UFM1 E3 ligase.

A. Comparison of size exclusion chromatography profiles of UFL1 expressed alone (Red) and co-expressed UFL1/UFBP1 complex (Black) run under identical buffer conditions on a HiLoad™ Superdex 10/300 gl column. Molecular weight standards are shown in grey. Fractions corresponding to each peak

958 were collected and analysed on 4-12% denaturing SDS-PAGE which is shown
959 below.

960 **B.** Mass photometry analysis of co-purified UFL1/UFBP1 complex. The theoretical
961 and experimental molecular weights are indicated above.

962 **C.** Immunoblot comparing UFL1 autoUFMylation *(Top)* and UFM1 chain synthesis
963 *(Middle)* in the presence of UFL1 expressed alone and in complex with UFBP1.
964 *(Bottom)* Assays to monitor UFMylation of substrates using purified TRIP4 in
965 the presence of UFL1 alone and UFL1/UFBP1 complex. Reaction products
966 were run on a 4-12% SDS-PAGE gel and analysed by immunoblotting using
967 indicated antibodies.

968 **D.** Immunoblot showing formation of free UFM1 chains in the presence and
969 absence of UFL1/UFBP1. *(Bottom)* Schematic representation of the linkage
970 composition of di-UFM1 chains obtained from LC-MS/MS analysis.

971 **E.** *In vitro* UFMylation assay in the presence of Lys to Arg (K-R) and lysine
972 less(K0) mutants of UFM1 to check for polyUFMylation *(top)* and UFL1
973 autoUFMylation *(bottom)*.

974 **F.** *In vitro* UFMylation assay to check for formation of di-UFM1 chains in the
975 presence of single Lys and Lys less mutants of UFM1.

976

977

Figure 3

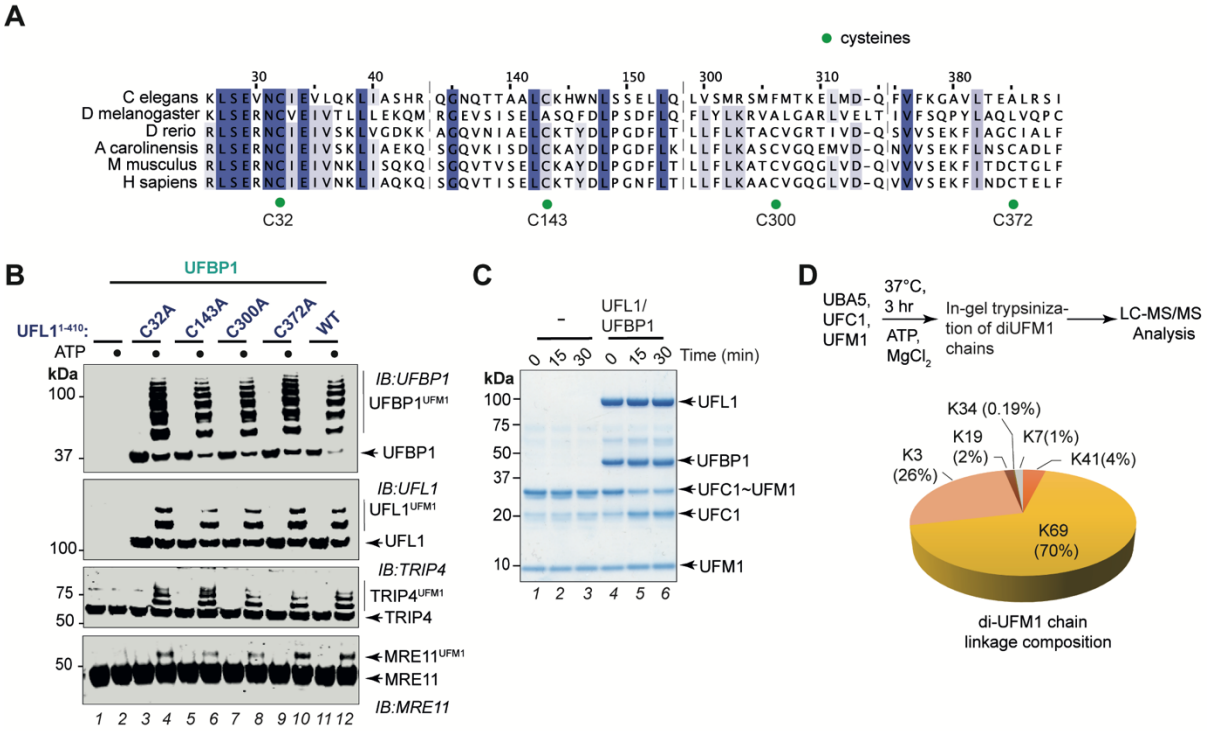

978
979

980 **Figure 3: - UFL1/UFBP1 is a scaffold type E3 ligase**

981 **A.** Multiple sequence alignment of 1-410 a.a. region of UFL1 from various
982 organisms to highlight the degree of conservation of cysteine residues in this
983 region.

984 **B.** Immunoblot showing *in vitro* UFMylation assays in the presence of C to A
985 mutants of UFL1 to check for UFBP1 UFMylation *(top)*, UFL1 autoUFMylation
986 *(middle)* and substrate UFMylation *(bottom)*.

987 **C.** Coomassie stained SDS-PAGE gel showing discharge assays in the presence
988 and absence of full length UFL1/UFBP1 complex. Charged UFC1 was
989 incubated with lysine (50 mM) in the presence and absence of full length
990 UFL1/UFBP1 complex and analysed for discharge on a 4-12% SDS PAGE gel
991 under non-reducing conditions.

992 **D.** Graphical representation showing the composition of linkage forms of di-UFM1
993 chains formed by minimal reconstitution of UBA5 and UFC1.

994
995
996

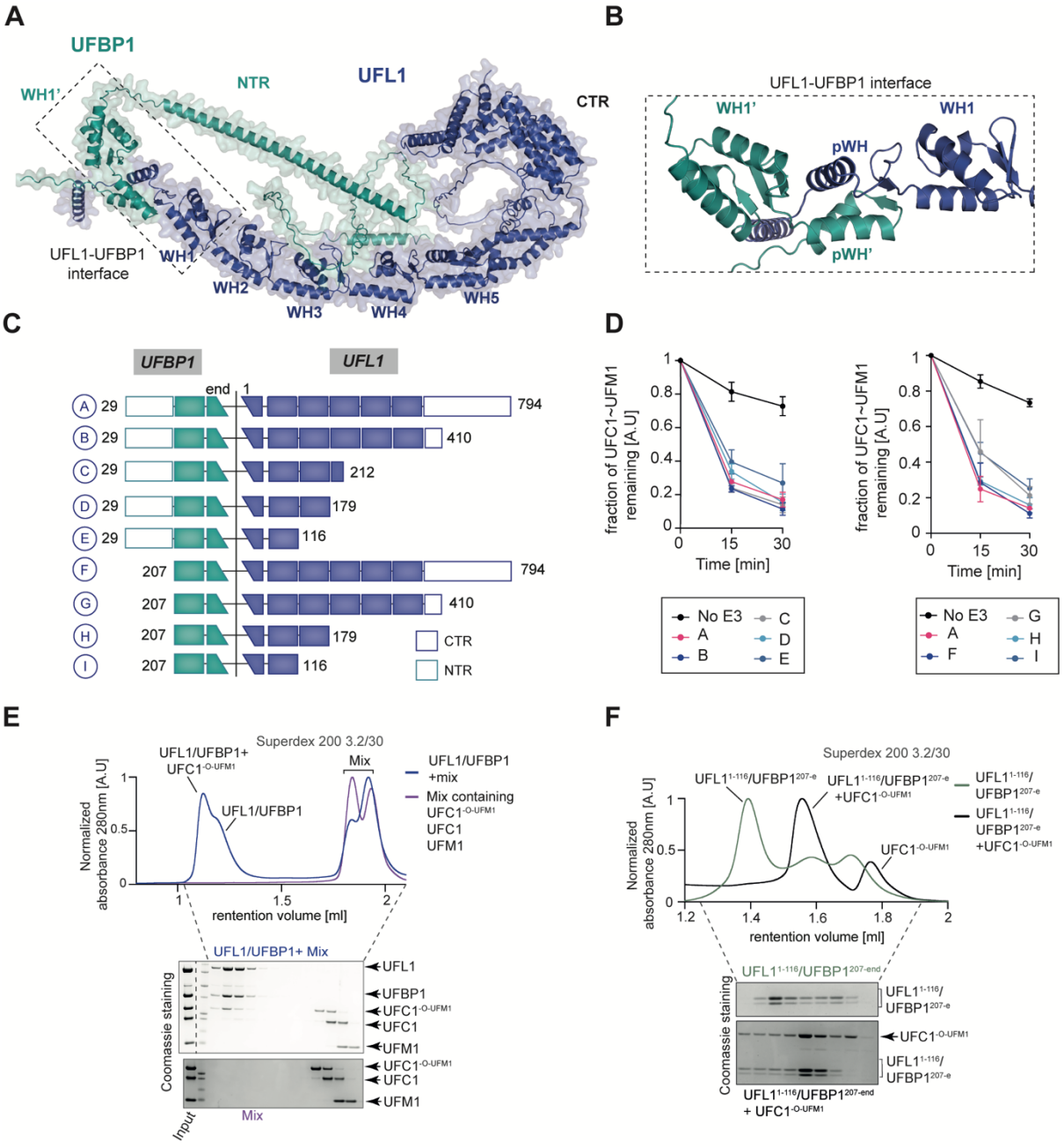
A
UFBP1
WH1'
NTR
UFL1
CTR
UFL1-UFBP1 interface
WH1
WH2
WH3
WH4
WH5
B
UFL1-UFBP1 interface
WH1'
WH1
pWH
pWH'
C
UFBP1
UFL1
end
1
29
207
794
410
212
179
116
CTR
NTR
D
fraction of UFC1~UFM1 remaining [A.U]
Time [min]
No E3
A
B
C
D
E
F
G
H
I
E
Superdex 200 3.2/30
UFL1/UFBP1+ UFC1-O-UFM1
UFL1/UFBP1
Mix
UFL1/UFBP1 +mix
Mix containing UFC1-O-UFM1 UFC1 UFM1
Normalized absorbance 280nm [A.U]
rentention volume [ml]
UFL1/UFBP1+ Mix
Coomassie staining
UFL1
UFBP1
UFC1-O-UFM1
UFC1
UFM1
Input
Mix
F
Superdex 200 3.2/30
UFL1 1-116/UFBP1 207-e
UFL1 1-116/UFBP1 207-e +UFC1-O-UFM1
UFC1-O-UFM1
UFL1 1-116/ UFBP1 207-e
UFL1 1-116/ UFBP1 207-e +UFC1-O-UFM1
Normalized absorbance 280nm [A.U]
rentention volume [ml]
UFL1 1-116/UFBP1 207-end
Coomassie staining
UFL1 1-116/ UFBP1 207-e
UFC1-O-UFM1
UFL1 1-116/UFBP1 207-end + UFC1-O-UFM1
G
Di-UFM1 Synthesis
E3:
ATP
kDa
10
di-UFM1
IB:UFM1
UFM1
H
Histone H4
20
H4UFM1
H4
IB:H4
I
Histone H4
20
H4UFM1
H4
IB:H4

1001 **Figure 4: - UFL1/UFBP1 complex functions as a scaffold type E3 ligase**

1002 **A.** Cartoon representation of predicted full length human UFL1/UFBP1 complex
1003 using Alphafold. UFL1 and UFBP1 are shown in blue and teal colors
1004 respectively. The dimeric interface of UFL1 and UFBP1 is highlighted in the
1005 dotted box. WH: Winged helix; NTR: N-terminal region; CTR: C-terminal region

1006 **B.** Enlarged view of the dimeric interface of UFL1/UFBP1 complex shown to
1007 highlight the formation of full WH domain bridged by two partial winged helix
1008 domains of UFL1 (blue) and UFBP1 (teal).

1009 **C.** Schematic representation of UFL1/UFBP1 constructs with different domain
1010 boundaries to identify the minimal catalytic region of UFL1/UFBP1 complex
1011 required for aminolysis.

1012 **D.** Quantitative representation of Lysine discharge assays to identify the minimal
1013 boundaries of UFL1 and UFBP1 required for activation of UFC1 (n=3,
1014 mean±SD).

1015 **E.** SEC elution profiles showing that full length UFL1/UFBP1 complex interacts
1016 specifically with charged E2. UFL1/UFBP1 complex was incubated with UFC1^{-}
1017 $^{O\text{-}UFM1}$ at a 1:1 molar ratio for 20 min at 4°C and loaded on a Superdex 200
1018 Increase 3.2/300 column. The fractions corresponding to each peak were
1019 collected and separated on a 4-12% SDS PAGE gel followed by Coomassie
1020 staining.

1021 **F.** Minimal catalytic region is sufficient for interaction with charged UFC1. UFL1$^{(1-}$
1022 $^{179)}$/UFBP1$^{(1-116)}$ complex was incubated with UFC1$^{-O\text{-}UFM1}$ at the molar ratio of
1023 1:1 for 20 min at 4°C and analysed by analytical size exclusion chromatography
1024 as described in E).

1025 **G.** *In vitro* UFMylation assay to monitor formation of free di-UFM1 chains in the
1026 presence of UFL1/UFBP1 complexes bearing different domain boundaries.

1027 **H.** Substrate UFMylations assays to check for UFMylation of purified Histone H4
1028 in the presence of different UFL1/UFBP1 truncations.

1029 **I.** Role of UFBP1 in substrate UFMylation. *(Top)* Comparison of UFMylation
1030 activities of UFL1/UFBP1$^{29\text{-}end}$ and UFL1/UFBP1$^{207\text{-}end}$ using Histone H4.
1031 *(Bottom)* Comparison of UFMylation activities of UFL1$^{1\text{-}179}$/UFBP1$^{29\text{-}end}$ and
1032 UFL1$^{1\text{-}179}$/UFBP1$^{207\text{-}end}$ using Histone H4.

Figure 5

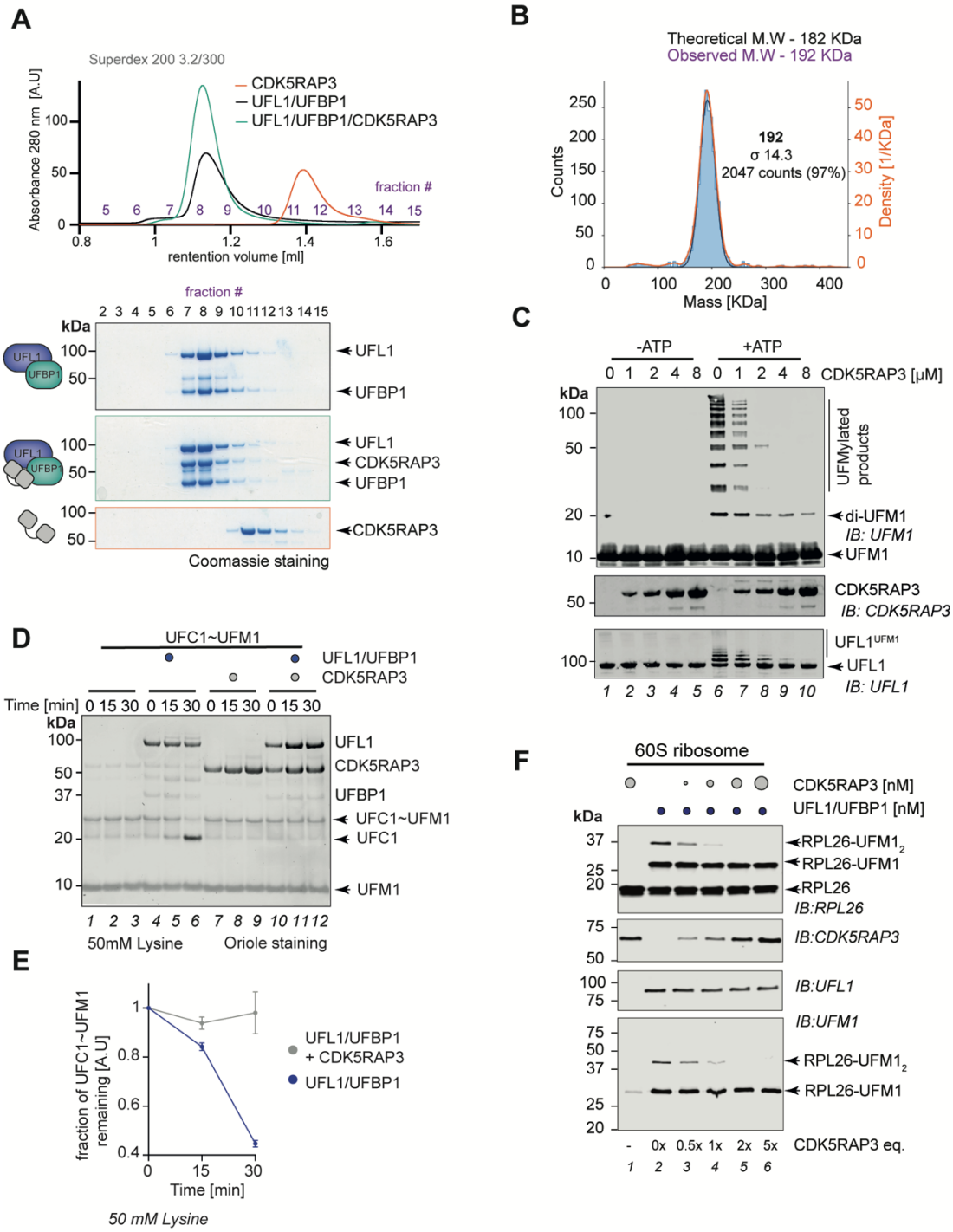

Figure 5: - CDK5RAP3 inhibits E3 ligase activity of UFL1/UFBP1 *in vitro*

A. CDK5RAP3 forms a complex with UFL1/UFBP1 *in vitro*. 30 μg of UFL1/UFBP1 was mixed with 15 μg of CDK5RAP3 and loaded on an analytical gel filtration column. (Bottom) Fractions were collected and analysed on 4-12% SDS PAGE and visualized by Coomassie staining.

1040 **B.** Mass photometry analysis showing the experimental molecular weight of
1041 UFL1/UFBP1/CDK5RAP3 complex.
1042 **C.** *In vitro* UFMylation assay in the presence of increasing concentrations of
1043 CDK5RAP3 to monitor the E3 ligase activity of UFL1/UFBP1 complex. The
1044 reaction products were run on a 4-12% SDS-PAGE gel and immunoblotting
1045 was performed using indicated antibodies.
1046 **D.** Lysine discharge assays to check for activation of UFC1 by UFL1/UFBP1 in the
1047 presence and absence of CDK5RAP3. The reaction products were run on a 4-
1048 12% SDS PAGE and visualized by Oriole staining.
1049 **E.** Quantification of discharge of UFM1 from UFC1 in the presence and absence
1050 of CDK5RAP3 as seen in E). n=3, mean ±SD.
1051 **F.** Substrate UFMylation assays using purified 60S Ribosomes in the presence of
1052 increasing concentration of CDK5RAP3. Reaction was performed for 10 min,
1053 stopped by addition of SDS Loading dye and analysed on an SDS-PAGE gel
1054 under reducing conditions followed by Immunobloting using indicated
1055 antibodies.
1056

Figure 6

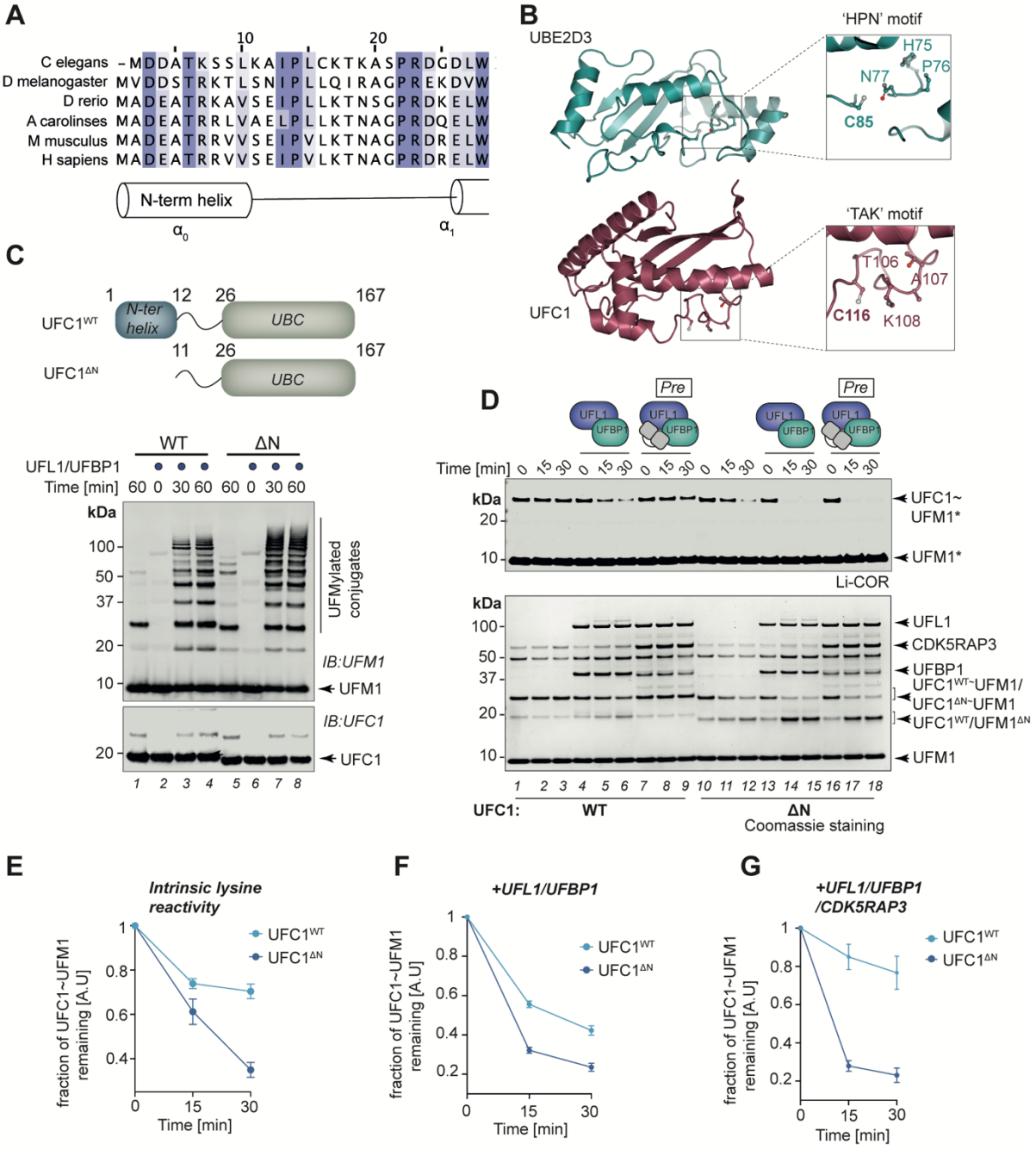

Figure 6:- Role of the N-terminal helix of UFC1 in UFMylation

A. Multiple sequence alignment of UFC1 homologs from various organisms. A graphical representation of the secondary structure is extracted from the crystal structure of UFC1 (PDB ID:2Z6O)

B. Crystal structures of UBE2D3 (PDB ID:5EGG) and UFC1 (PDB ID:2Z6O) are shown in cartoon representation. *(Inset)* Catalytic cysteines and critical

1065 residues required for catalytic activity of UBE2D3 (green) and UFC1(dark red)
1066 are labelled and shown in ball and stick representation.

1067 **C.** *In vitro* UFMylation assays in the presence of Wild type UFC1 ($UFC1^{WT}$) and
1068 UFC1 lacking the N-terminal helix ($UFC1^{\Delta N}$). Schematic representation of
1069 domain features of $UFC1^{WT}$ and $UFC1^{\Delta N}$ is shown above.

1070 **D.** Assay to compare Lys discharge activities of $UFC1^{WT}$ and $UFC1^{\Delta N}$ on its own,
1071 in the presence of UFL1/UFBP1 or in the presence of preassembled
1072 UFL1/UFBP1/CDK5RAP3 complex. Top gel: LiCOR scan of fluorescently
1073 labelled UFM1(UFM1*); bottom gel – Coomassie stained (Representative of
1074 three independent experiments).

1075 **E.** Quantitative analysis of the intrinsic Lys reactivity (Lysine 25 mM) of $UFC1^{WT}$
1076 and in $UFC1^{\Delta N}$ in the absence of E3 ligase.

1077 **F.** Quantitative analysis of Lys reactivity of $UFC1^{WT}$and in $UFC1^{\Delta N}$ in the presence
1078 of UFL1/UFBP1.

1079 **G.** Quantitative analysis of Lys reactivity of $UFC1^{WT}$and in $UFC1^{\Delta N}$ in the the
1080 presence of preassembled UFL1/UFBP1/CDK5RAP3. E – G: n=3, mean ±SD.

1081
1082

1083 **Supplementary Material**

1084

1085

Figure S1

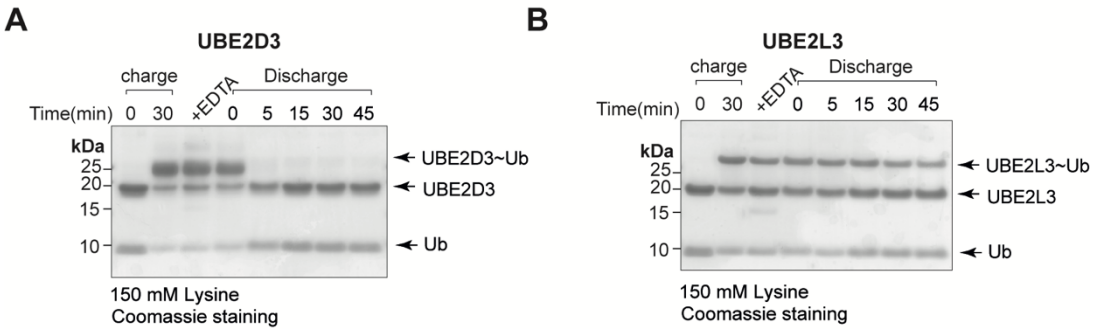

1086
1087

1088 **Figure S1: Analysis of E2 discharge**

1089 **A.** & **B.** Time-dependent analysis of discharge of Ubiquitin from UBE2D3 and
1090 UBE2L3 in the presence of 150 mM.

1091

Figure S2

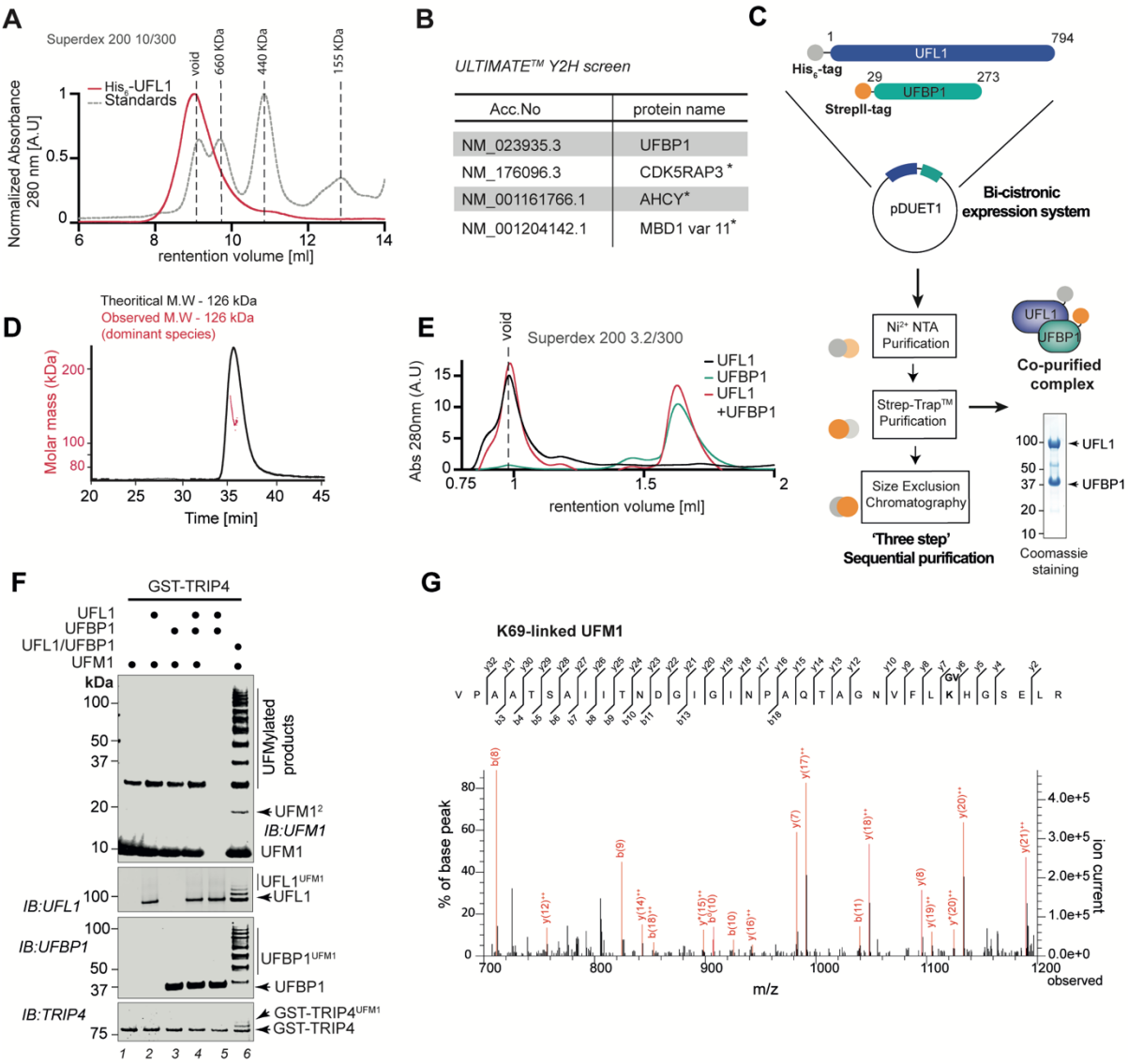

Figure S2: UFL1 is only active in the presence of co-expressed UFBP1

A. Size exclusion chromatography profile of UFL1 run on Superdex 200 Increase 10/300gl column (shown in red). Overlay of chromatogram of molecular weight standards of different sizes (shown in grey) run under same buffer conditions.

B. Results obtained from ULTIMATE Y2H™ screening (Hybrigenics) for binary interactions with UFL1. Asterisk denotes protein hits obtained with low confidence.

C. Schematic describing the strategy for co-expression and purification of UFL1/UFBP1 complex.

1104 **D.** SEC-MALS analysis of UFL1/UFBP1 complex. The theoretical and observed
1105 molecular weights are indicated.
1106 **E.** Analytical gel filtration chromatography analysis of UFL1/UFBP1 complex and
1107 its subunits run on Superdex 200 3.2/300.
1108 **F.** UFBP1 does not activate UFL1 when added exogenously. *In vitro* UFMylation
1109 assays to compare the E3 ligase activity of UFL1 and UFBP1 expressed alone
1110 and together as a complex. 0.25 μM UBA5, 5 μM UFC1 and 10 μM UFM1 was
1111 incubated with 1 μM UFL1 or 1 μM UFBP1 or 1 μM UFL1/UFBP1 complex for
1112 1 h at 37°C in the presence of 50 mM HEPES 7.5, 0.5 mM DTT, 10 mM $MgCl_2$
1113 and 10 mM ATP. The reaction was stopped by addition of 3x SDS loading dye
1114 and run on a 4-12% denaturing SDS PAGE gel under reducing conditions and
1115 immunoblotting was performed using indicated antibodies.
1116 **G.** MS^2 spectra showing the peptide derived from *in vitro* UFMylation assay
1117 showing the VG-remnant on K69 of UFM1.
1118

Figure S3

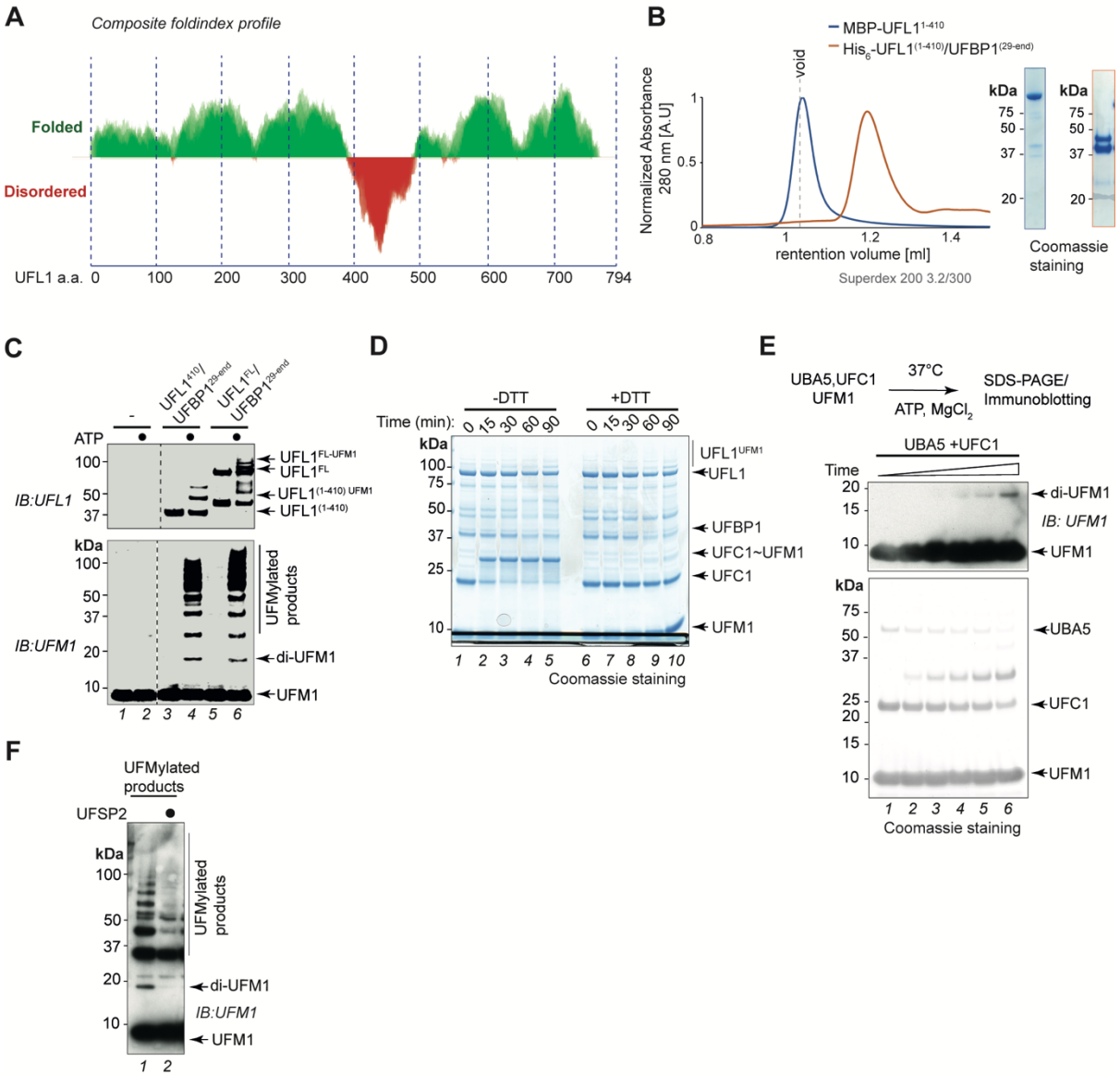

Figure S3: Mode of UFMylation by UFL1/UFBP1 complex

A. Composite Foldindex profile of UFL1 showing folding propensity of different regions of UFL1 to aid in construct design for soluble protein expression.

B. Size exclusion chromatography profile of MBP-UFL1$^{1-410}$ (dark blue) and His$_6$-UFL1$^{1-410}$/UFBP1^{29-end}(orange) run on Superdex 200 3.2/300 column (shown in red). Approximately 20 μgs of sample was run on a Superdex 200 3.2/300 analytical gel filtration column and UV traces measured at 280 nm were recorded and analysed. (Right) Coomassie stained gel showing the purity of the proteins.

1130 **C.** *In vitro* UFMylation assay to check for E3 ligase activity of UFL1$^{1-410}$/UFBP1^{29-end}. Full length UFL1/UFBP1 complex is used as a positive control.

1132 **D.** Time course assay to check for transthiolation activity of UFL1. Reaction products were analysed on a 4-12% SDS PAGE gel under reducing and non-reducing conditions.

1135 **E.** *In vitro* UFMylation assays to check for formation of di-UFM1 chains in the by minimal reconstitution in the presence UBA5 and UFC1 alone.

1137 **F.** Immunoblot to check for the presence of UFM1 chains with and without treatment of UFSP2. *In vitro* UFMylation products generated as shown in E was incubated with UFSP2 and analysed by immunoblotting using anti-UFM1 antibody to check for the disspearence of polyUFMylated products especially di-UFM1.

1142

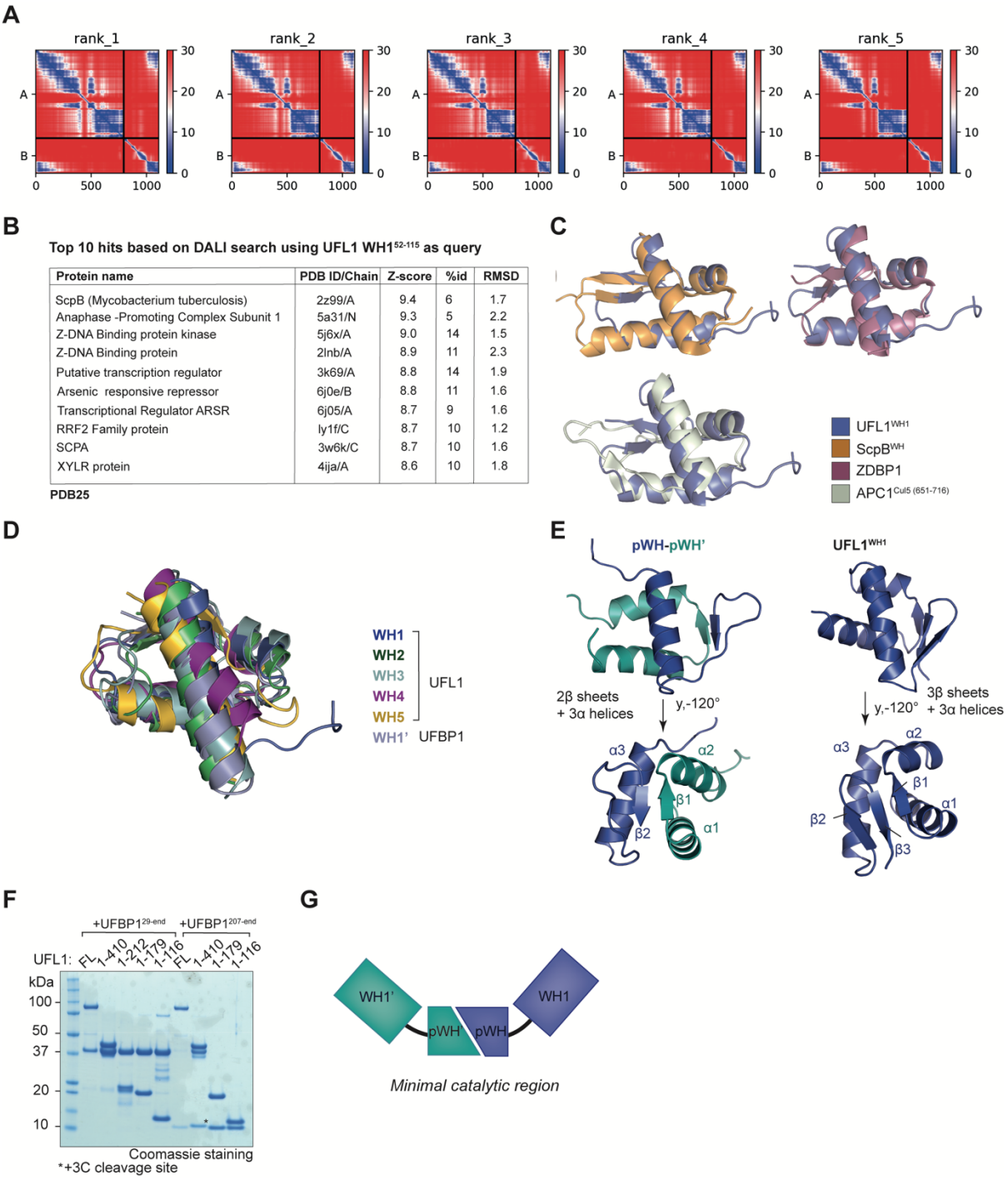

Figure S4: - Identifying the minimal ligase domain of UFL1/UFBP1 complex

A. Predicted Aligned Error (PAE) scores of predicted UFL1/UFBP1 models using AlphaFold.

B. List of structurally similar proteins from the PDB25 database predicted using UFL1 WH1(52-115) domain as query structure using DALI server.

C. Overlaid structures of Winged helix 1(WH1) domain of UFL1(52-115) and top three hits obtained from DALI search shown in cartoon representation.

1152

1153 **D.** Superposition of the winged helix (WH) domains of UFL1 and UFBP1.

1154 **E.** Comparison of composite winged helix domain formed by two hemi WH
1155 domains of UFL1 (pWH) and UFBP1 (pWH') with the WH1 domain of UFL1.

1156 **F.** Coomassie stained gel showing purity of different UFL1/UFBP1 truncations.

1157 **G.** Schematic showing the tandem WH domains which constitute the minimal
1158 ligase domain.

1159

1160

Figure S5

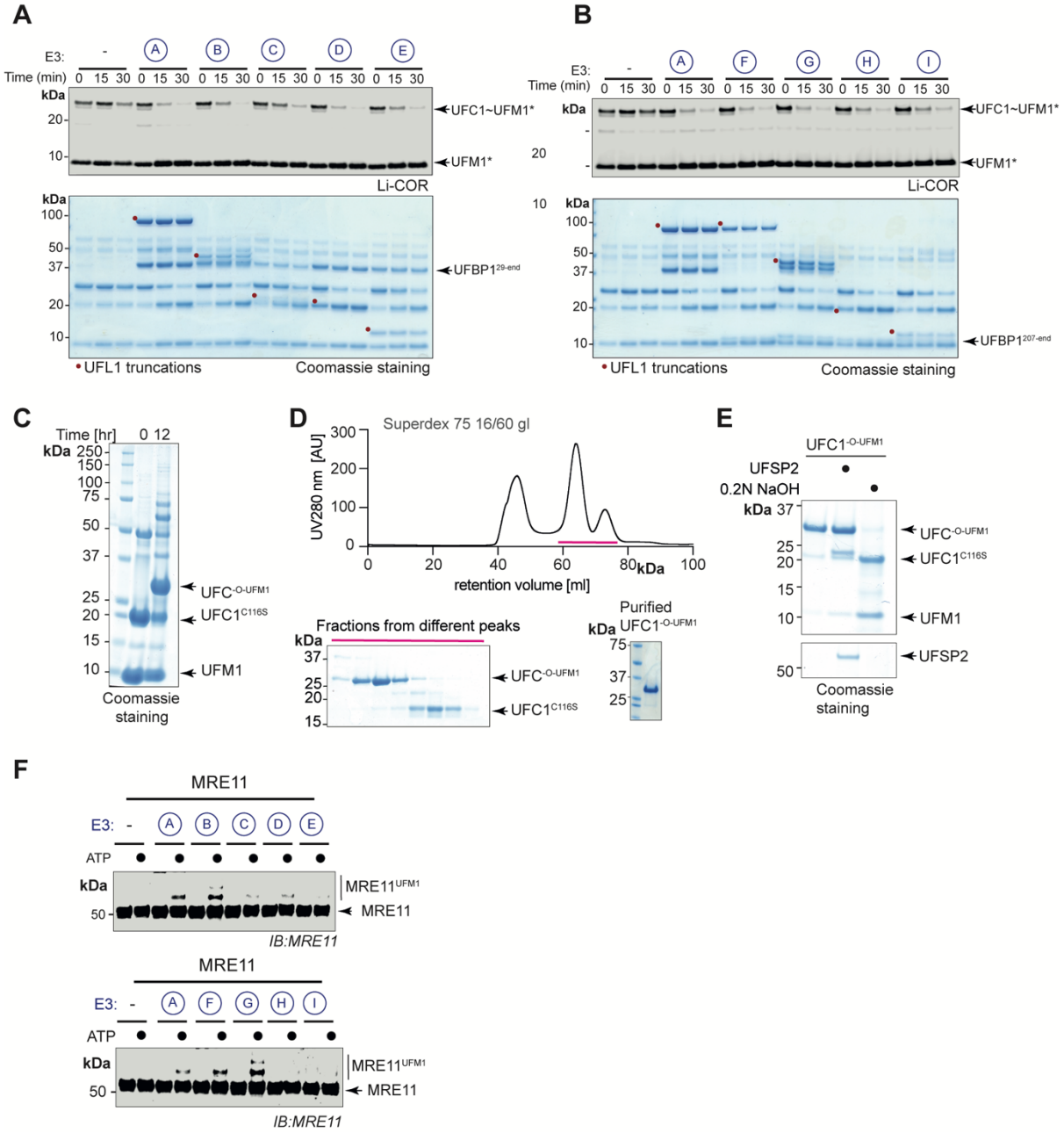

Figure S5: - UFL1/UFBP1 E3 ligase complex binds to UFC1~UFM1 and induces aminolysis

A. Lysine discharge assays to check for activation of UFC1 in the presence of different UFL1 truncations. Top gel: LiCOR scan of fluorescently labelled UFM1(UFM1*); bottom gel – Coomassie stained (Representative of three independent experiments).

B. Lysine discharge assays as in A) in the absence of NTR of UFBP1(representative of 3 independent experiments).

1171 **C.** Coomassie stained gel showing analysis of *in vitro* UFMylation reaction
1172 products to check for the formation of stable oxy-ester linked UFC1-UFM1
1173 conjugate ($UFC1^{-O-UFM1}$).
1174 **D.** Chromatogram obtained from SEC analysis using HiLoad™ Superdex 75
1175 16/60pg column. (Bottom left) The fractions collected were run on an SDS-
1176 PAGE gel to identify fractions that contained pure $UFC1^{-O-UFM1}$. (Bottom right)
1177 Coomassie stained gel showing analysis of purified $UFC1^{-O-UFM1}$ product to
1178 check for homogeneity.
1179 **E.** Quality check to analyse if UFC1-UFM1 conjugate is linked through an oxy-
1180 ester linkage by alkaline hydrolysis.
1181 **F.** Substrate UFMylations assays to check for UFMylation of MRE11 in the
1182 presence of different UFL1/UFBP1 truncations.
1183
1184
1185

Figure S6

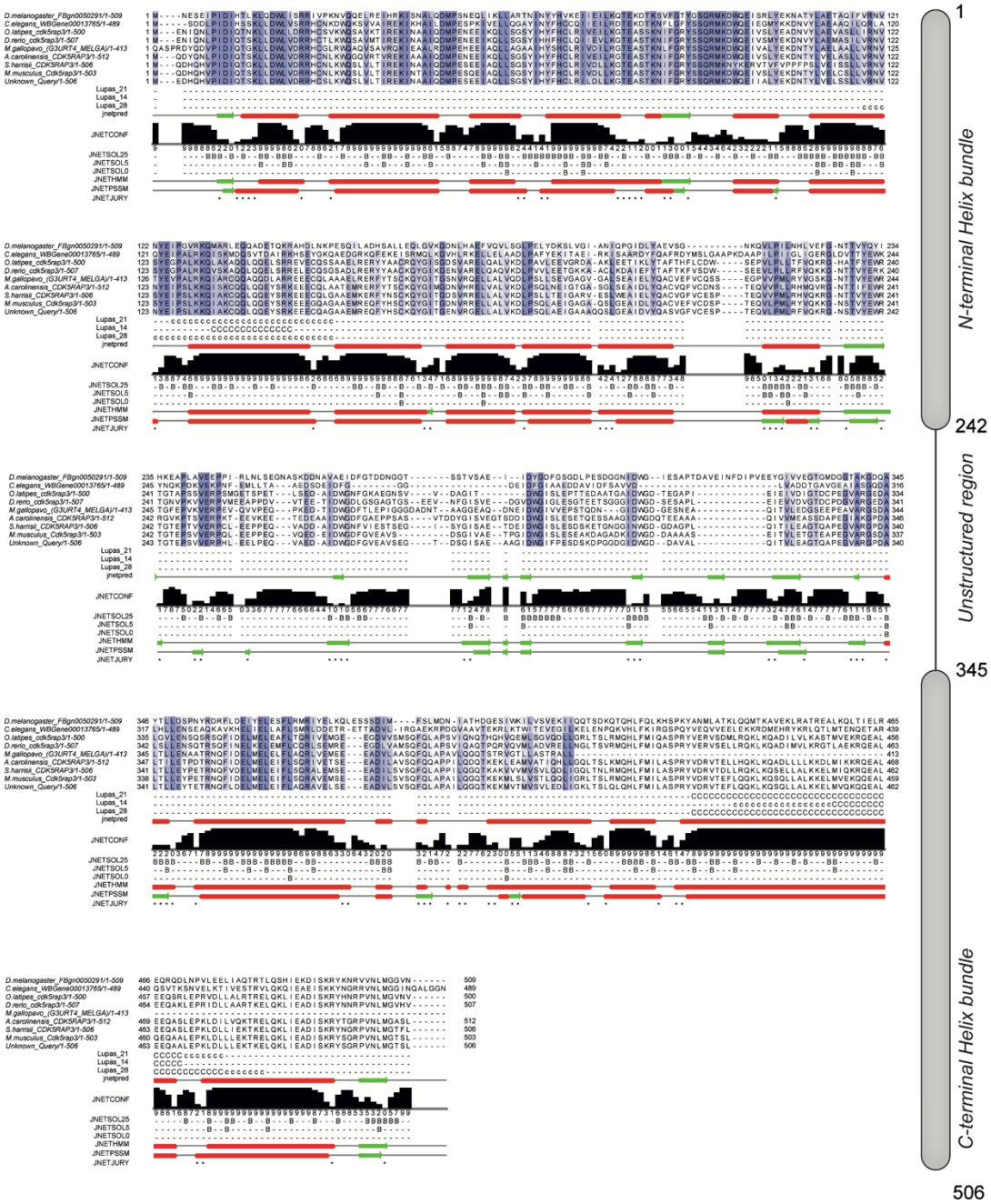

Figure S6: - Sequence and secondary structure analysis of CDK5RAP3

A. (Left) Multiple sequence alignment of CDK5RAP3 homologs showing predicted secondary structure features using JPred^{TM} secondary structure program module from Jalview 2.11.1.7.**(Right)** Schematic showing predicted secondary structure features of CDK5RAP3.

Figure S7

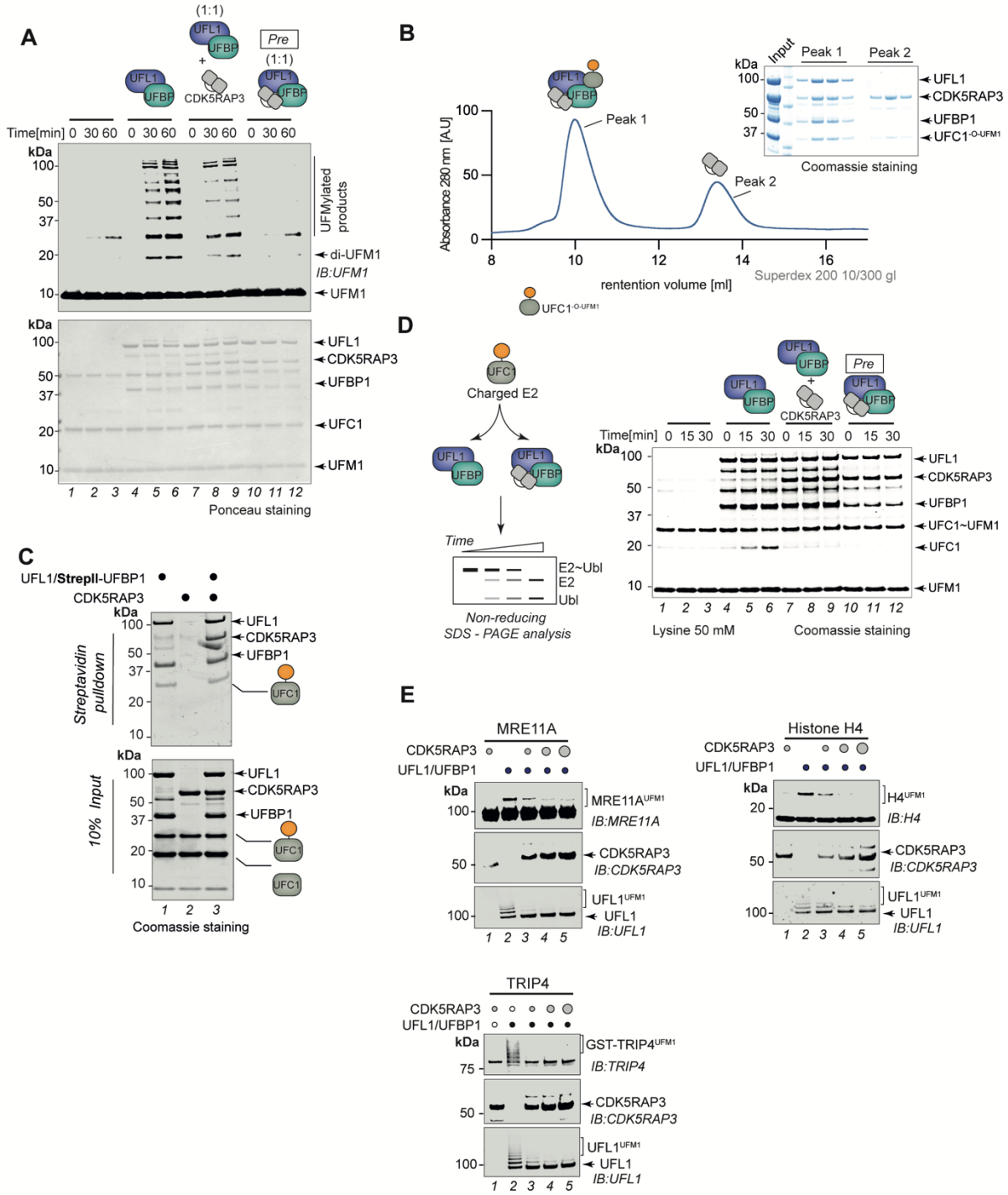

Figure S7:- Role of CDK5RAP3 in UFMylation

A. *In vitro* UFMylation assay to compare the E3 ligase activity of UFL1/UFBP1 mixed with CDK5RAP3 and preassembled ternary E3 ligase complex containing UFL1/UFBP1/CDK5RAP3. Ponceau-stained membrane is showed below to indicate the amounts of reaction components used in the assay.

1201 **B.** UV traces of gel filtration chromatogram showing co-migration of
1202 (UFL1/UFBP1)/CDK5RAP3/UFC1$^{-O-UFM1}$ complex. Approximately, 200 μl of
1203 sample containing (UFL1/UFBP1)/CDK5RAP3/UFC1$^{-O-UFM1}$ in the molar ratio
1204 of 1:1.5:3 was mixed and incubated at 4°C for 1 h and loaded onto a Superdex
1205 200 10/300 gl column. The fractions were collected and analysed on a 4-12%
1206 SDS PAGE and visualized by Coomassie staining.
1207 **C.** Pulldown assay to check for interaction of UFL1/UFBP1 with charged UFC1 in
1208 the presence of absence of CDK5RAP3. Around 10 μM of Untagged UFC1 and
1209 10 μM OF UFC1-O-UFM1 were mixed with 5 μM of UFL1/UFBP1 complex in
1210 the presence and absence of CDK5RAP3.
1211 **D.** Lysine discharge assays to check for UFC1 discharge in the presence of
1212 UFL1/UFBP1 mixed with CDK5RAP3 and preassembled
1213 UFL1/UFBP1/CDK5RAP3 complex. The reaction products were run on a 4-
1214 12% SDS PAGE analysis and visualized by Coomassie staining.
1215 **E.** *In vitro* UFMylation assay to monitor UFMylation of purified substrates namely
1216 TRIP4, MRE11A and Histone H4.
1217
1218

Figure S8

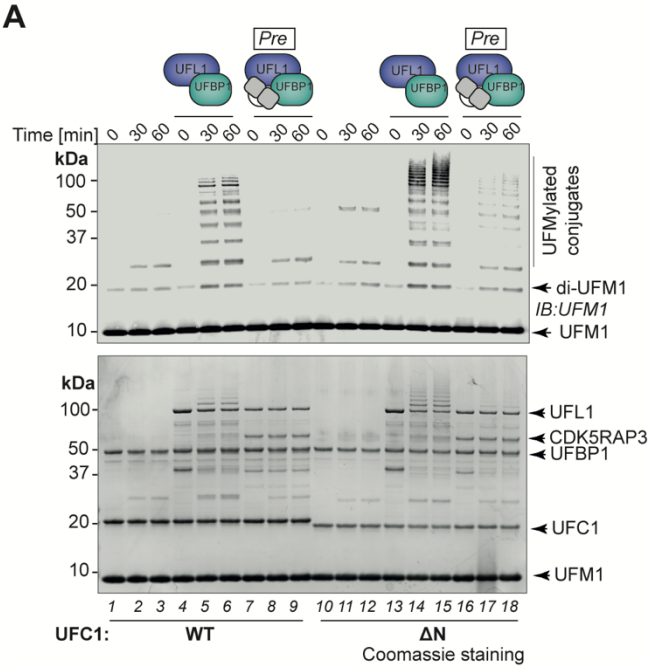

Figure S8:- Role of the N-terminus of UFC1 in regulating UFMylation

A. *In vitro* UFMylation assay to compare the activites of UFC1^{WT} and UFC1$^{\Delta N}$ on its own, in the presence of UFL1/UFBP1 or in the presence of preassembled UFL1/UFBP1/CDK5RAP3 complex (Representative of three independent experiments).

1225 **Table S1**

REAGENT or RESOURCE	SOURCE	IDENTIFIER
Antibodies		
Anti-UFM1	Abcam	ab109305
Anti-UBA5	Universal Biologicals	A304-115A-T
Anti-UFC1	Abcam	ab189252
Anti-UFL1	Abcam	ab227506
Anti-UFBP1	Abcam	ab99121
Anti-CDK5RAP3	Bethyl Laboratories	A300-870A
Anti-TRIP4	Bethyl Laboratories	A300-203A-M
Anti-MRE11A	Bethyl Laboratories	A300-181A
Anti-H4	Abcam	ab10158
Anti-RPL26	Bethyl laboratories	A300-686A-M
Anti-rabbit IgG, HRP-linked Antibody	CST	70745
IRDye 800CW anti-Rabbit	Li-COR	926-32211
IRDye 680CW anti-Rabbit	Li-COR	926-68071
Chemicals and other consumables		
IRDye® 800CW Maleimide	Li-COR	929-80020
Phusion® High-Fidelity DNA Polymerase	New England Biolabs	M0530
Q5® site directed mutagenesis kit	New England Biolabs	E0554S
QIAGEN Plasmid Mini kit	Qiagen Ltd.	12123
dNTPs	Thermo Fisher	R0181
4-(2-aminoethyl) benzene sulphonyl fluoride hydrochloride (AEBSF)	Apollo Scientific	BIMB2003
Benzamidine	Apollo Scientific	1670-14-0
Tris (2-carboxyethyl) phosphine hydrochloride (TCEP)	Apollo Scientific	BIT0122
Isopropyl thio-β-D galactoside (IPTG)	Formedium	IPTG100
Dithiothreitol (DTT)	Formedium	DTT100
Roche cOmplete EDTA-free protease inhibitor cocktail	Roche	11873580001
L-Lysine monohydrochloride	Sigma-Aldrich	L8662-25G
L-Serine	Merck	S4211-25G
L-Threonine	Merck	T0387-10MG
L-Cysteine	Sigma-Aldrich	168149

L-Arginine	Sigma-Aldrich	A8094-100G
Adenosine 5'-triphosphate (ATP)	Apollo Scientific	BIB3003
Ni^{2+}NTA agarose	Amintra, Abcam	ab270549
Glutathione SH-4B sepharose	Amintra, Abcam	Ab270237
Amylose Resin	New England Biolabs	E8021L
HisTrap FF columns	GE Healthcare Life Sciences	17525501
StrepTrap columns	GE Healthcare Life Sciences	28907547
Strep-Tactin Sepharose resin	IBA Lifesciences	2-1201-010
3C (PreScission) protease	MRC PPU Reagents and Services	DU34905
TEV protease	MRC PPU Reagents and Services	DU6811
Recombinant proteins		
MBP-3C-UFL1$^{1-410}$	This Study	DU67192
His_6-3C-UFL1^{FL}	This Study	DU63471
GST-3C-UFL1^{FL}	This Study	DU47296
mMBP-3C-DDRGK1	This Study	DU59678
His_6-3C-UBA5	This Study	DU32106
GST-3C-UFC1	This Study	DU55394
GST-3C-UFC1^{C116S}	This Study	DU59294
His_6-3C-UFC1^{WT}	This Study	DU59469
His_6-3C-UFC1$^{\Delta N}$	This Study	TBD
GST-3C-UFM1$^{(1-83)\ K0}$	This Study	DU59472
GST-3C-UFM1$^{(1-83)\ K3R}$	This Study	DU59442
His_6-3C-UFM1$^{(1-83)\ K7R}$	This Study	DU59443
His_6-3C-UFM1$^{(1-83)\ K19R}$	This Study	DU59444
His_6-3C-UFM1$^{(1-83)\ K34R}$	This Study	DU59445
His_6-3C-UFM1$^{(1-83)\ K41R}$	This Study	DU59562
His_6-3C-UFM1$^{(1-83)\ K69R}$	This Study	DU59446
His_6-TEV-Cys-UFM1$^{(1-83)}$	This Study	DU55017
His_6-3C-UFM1$^{(1-83)\ K3\ only}$	This Study	TBD
His_6-3C-UFM1$^{(1-83)\ K7\ only}$	This Study	TBD
His_6-3C-UFM1$^{(1-83)\ K19\ only}$	This Study	TBD
His_6-3C-UFM1$^{(1-83)\ K34\ only}$	This Study	TBD

His_6-3C-UFM1$^{(1-83)\ K41\ only}$	This Study	TBD
His_6-3C-UFM1$^{(1-83)\ K69\ only}$	This Study	TBD
His_6-TEV-UFL1^{FL} /StrepII 3C DDRGK1^{29-end}	This Study	DU63479
His_6-TEV-UFL1$^{(1-410)}$ /StrepII-3C-DDRGK1^{29-end}	This Study	DU66224
His_6-TEV- UFL1$^{(1-212)}$ /StrepII-3C-DDRGK1^{29-end}	This Study	DU66218
His_6-TEV-UFL1$^{(1-179)}$ /StrepII-3C-DDRGK1^{29-end}	This Study	TBD
His_6-TEV-UFL1$^{(1-116)}$ /StrepII-3C-DDRGK1^{29-end}	This Study	TBD
His_6-TEV-UFL1^{FL} /StrepII-3C-DDRGK1$^{207-end}$	This Study	TBD
His_6-TEV-UFL1$^{(1-410)}$/StrepII-3C-DDRGK1$^{207-end}$	This Study	TBD
His_6-TEV-UFL1$^{(1-179)}$/StrepII-3C-DDRGK1$^{207-end}$	This Study	TBD
His_6-TEV-UFL1$^{(1-116)}$/StrepII-3C-DDRGK1$^{207-end}$	This Study	TBD
His_6-TEV-UFL1$^{C32A(1-410)}$/StrepII-3C-DDRGK1 $^{29-end}$	This Study	DU66308
His_6-TEV-UFL1$^{C143A(1-410)}$/StrepII-3C-DDRGK1 $^{29-end}$	This Study	DU66287
His_6-TEV-UFL1$^{C300A(1-410)}$/StrepII-3C-DDRGK1 $^{29-end}$	This Study	DU66288
His_6-TEV-UFL1$^{C374A(1-410)}$/StrepII-3C-DDRGK1 $^{29-end}$	This Study	DU66289
His_6-TEV-UFL1$^{(1-410)C32A,C143A,C300A,C372A}$ /StrepII-3C-DDRGK $^{29-end}$	This Study	DU66290
MBP-3C-CDK5RAP3	This Study	DU59674
His_6-3C-MRE11$^{(1-411)}$	This Study	DU66124
GST-TEV-TRIP4	This Study	DU59564
UBE1$^{(2-1058)}$	MRC PPU Reagents and Services	DU3026
UBE2D3	MRC PPU Reagents and Services	DU15703
UBE2L3	MRC PPU Reagents and Services	DU3772

TBD – (To be decided)